Reply to comments by the editor and the referees

R. Rüfenacht, K. Hocke, N. Kämpfer

April 7, 2016

The present document contains the author's replies to all remarks by the editor and the referees after the first revision of the manuscript. The authors would like to thank the editor and the referees for their efforts related to this paper.

- red: editor's comments
- blue: referee's comments
- green: author's replies

Please look at the second set of comments from reviewer 1 (below) and either do as suggested or give a clear reason why not.

Main points

I reiterate that the authors have done well to address my points from the previous review and the paper now is solid. However, having reread the paper, I still do not have an idea for what observations are going into the ECMWF OA in the upper stratosphere and mesosphere as shown in figures 3,4,6 and 7. Information on what relevant observations there are and when they were included is required (say at 1hPa and above). The inclusion of new observations during an extended period of time can introduce sudden jumps in the time domain of climate fields (so in then light of the present analysis, these need to be checked). Perhaps the authors could supply the equivalent of figure 1, but for the ECMWF OA, in the Supplement.
After a thorough literature research and discussions with researches specialised in modeling we are quite sure that no overview document summarising all relevant observations assimilated in ECMWF's operational analysis. Such a paper only exists for the ERA-Interim re-analysis and has already been cited in the manuscript (Dee, 2011). To make the situation about the upper-altitude data assimilation in ECMWF more clear we added the following statement on page 35039 line 13: "The few observations assimilated at higher altitudes mainly originate from infrared radiation soundings (Engelen and Bauer, 2014; Dragani and McNally, 2013, and references therein)."
According to your suggestion we also added a figure showing the wind time series of the ECMWF operational analysis to the Supplement (Figure S2 with

reference in the main article on page 35039, line 21). The ECMWF time series do not show any jumps in the wind field.

Other point, the authors have chosen to retain the Lomb-Scargle theory in the paper. I suggest that the authors check the journal guidelines on mathematical typesetting. I (and probably most of the Journal's readers) do not recognise the usage of two symbols (e.g. the use of hashes in equation 4, and the caret symbol in equations 2 and 3).
For better understandability for readers who are not familiar with the notations of logical mathematics the meaning of the used symbols has been clarified in the text on page 35041 line 5: "In Eqs. (2) to (4) $\wedge$ and $\vee$ denote logical "and" and "or" while the cardinality operator # returns the number of elements of its argument."

Finally, I still do not like the use of "strato-mesospheric" in the title (middle atmosphere or stratosphere-mesosphere would be much better and are recognisable). Authors call on this one.
As our previous answer does not seem to be satisfactory to you we opted for a less concise and more descriptive title: "First continuous ground-based observations of long period oscillations in the vertically resolved wind field of the stratosphere and mesosphere"

Minor points

(35044, L27) "measurements"
Corrected, thank you.

(35045, L20) "...in detail." A reference to the spectral gravity wave scheme could also be added (e.g. Scinocca, 2003). The background to the gravity wave scheme used in the IFS model used in the Operational Analysis dataset can be found at http://www.ecmwf.int/sites/default/files/elibrary/2010/9233-part-iv-physical-processes.pdf
modified to "in detail". The authors do not want to introduce more speculations on possible reasons for the discrepancies between observations and model as no definite answer could be found. Therefore we do not deliver more details about the gravity wave parametrisation scheme here. A more exact description about the ECMWF model is provided in section 2.2. of the manuscript.

Also, perhaps the authors should replace "upward momentum transport" with upward transport of horizontal momentum from resolved and parametrised waves.
Modified to "upward transport of horizontal momentum".

(35046, L3) suggest: "and/or seasonally dependent" or "and/or seasonally constrained"
Modified to "and/or seasonally constrained"

(35047, L1) Capitalise Northern Hemisphere
Modified.

Manuscript prepared for Atmos. Chem. Phys. Discuss.
with version 2015/04/24 7.83 Copernicus papers of the LaTeX class copernicus.cls.
Date: 6 April 2016

First continuous ground-based observations of long period oscillations in ~~strato-/mesospheric~~ the vertically resolved wind ~~profiles~~field of the stratosphere and mesosphere

R. Rüfenacht, K. Hocke, and N. Kämpfer

Institute of Applied Physics, University of Bern, Bern, Switzerland

Correspondence to: R. Rüfenacht (rolf.ruefenacht@iap.unibe.ch)

Abstract

Direct measurements of middle-atmospheric wind oscillations with periods between 5 and 50 days in the altitude range between mid-stratosphere (5 hPa) and upper mesosphere (0.02 hPa) have been made using a novel ground-based Doppler wind radiometer. The oscillations were not inferred from tracer measurements, as the radiometer offers the unique capability of near-continuous horizontal wind profile measurements. Observations from four campaigns at high, mid and low latitudes with an average duration of 10 months have been analyzed. The dominant oscillation has mostly been found to lie in the extra-long period range (20–50 days), while the well-known atmospheric normal modes around 5, 10 and 16 days have also been observed. Comparisons of our results with ECMWF Operational Analysis data revealed remarkably good agreement below 0.3 hPa but discrepancies above.

1 Introduction

The dynamics of the middle atmosphere is characterized by waves and oscillations with distinct periods. An accurate representation of the middle-atmospheric dynamics can improve the forecast skills of numerical weather prediction models, especially on time scales beyond one week (e.g. Baldwin et al., 2003b, a; Charlton et al., 2004; Hardiman et al., 2011; Sigmond et al., 2013). Therefore validation of these models is needed also in the stratosphere and mesosphere in addition to tropospheric analyses. Thereby not only the correctness of the absolute values of the atmospheric parameters, but also the correct representation of their natural oscillations should be studied as such oscillations play an important role in the dynamics of the middle atmosphere.

Measurements of zonal and meridional wind are the most direct way to observe atmospheric dynamics. For studying long period oscillations long time series of continuous measurements are required. However, wind observations in the upper stratosphere and lower mesosphere are practically non-existent and the few measurements available are not present on a continuous basis (see Supplement Text S1).

Rocket soundings (e.g. National Research Council, 1966; Müllemann and Lübken, 2005) and the Doppler wind lidar at ALOMAR (Hildebrand et al., 2012; Baumgarten, 2010) have been used to retrieve vertical profiles of horizontal wind throughout the stratosphere and mesosphere. However the novel ground-based microwave wind radiometer WIRA (Rüfenacht et al., 2012, 2014) is the only instrument capable of providing wind observations between 35 and 70 km altitude (5 to 0.04 hPa) with time series satisfying the requirement of long term continuity. Presently, the published wind lidar data sets are too short for long period spectral analyses. The coarse time resolution of rocket soundings seems inadequate for the investigation of oscillations with periods shorter than approximatively 20 days. A rocket-sensed wind data set with 1–2 profiles per week has, however, been used by Keckhut (1995) in a study investigating the effect of the 27-day solar rotation period on middle atmospheric dynamics.

Oscillations of horizontal wind in the (upper) mesosphere/lower thermosphere (MLT) have been extensively studied using radar observations (e.g. Araújo et al., 2014; Day et al., 2012; Guharay et al., 2014; Luo et al., 2001, 2002). In the upper stratosphere and lower mesosphere region analyses of long period oscillations in the concentration of trace gases, such as ozone and water vapor, have been reported based on microwave radiometry (e.g. Hocke et al., 2013; Scheiben et al., 2014).

Here we present an analysis of oscillations in upper stratospheric and mesospheric horizontal wind profiles with periods between 5 and 50 days. We also compare results obtained from wind radiometer measurements to the Operational Analysis data from the European Centre for Medium-Range Weather Forecast model (ECMWF).

2 Data sets

2.1 Wind radiometer data

The Doppler WInd RAdiometer WIRA is a novel ground-based passive heterodyne receiver designed for the observation of horizontal wind profiles from the mid-stratosphere (5 hPa) to the mesopause (0.02 hPa) where no other application provides continuous time series of wind measurements. Wind profiles are determined by measuring Doppler shifts of the pressure broadened emission line of ozone at 142 GHz. The retrieval from the raw data is based on an optimal estimation inversion (Rodgers, 2000) of an atmospheric radiative transfer model implemented in the ARTS/QPACK software (Eriksson et al., 2011, 2005). Typical measurement uncertainties and vertical resolutions of the daily average wind profiles used in this study range from 10 to 20 $\mathrm{m\,s^{-1}}$ and from 10 to 16 km, respectively. However, as indicated by Rodgers (2000), features vertically spaced by less than 10 km can in many cases be recognized as individual peaks in the retrieved data, although their amplitudes are not independent. Detailed descriptions of the instrument and retrieval characteristics of WIRA have already been published (Rüfenacht et al., 2012, 2014).

A strength of microwave radiometers is their ability to take measurements during day and night and under overcast conditions. This strength, combined with low operation costs, allows for the recording of long continuous time series. The present study is based on measurements taken by WIRA at four different locations at high, mid and low latitudes: Sodankylä (67°22′ N/26°38′ E, October 2011–July 2012), Bern (46°57′ N/7°26′ E, September 2010–July 2011), Observatoire de Haute-Provence (43°56′ N/5°43′ E, November 2012–May 2013) and Observatoire du Maïdo on La Réunion (21°04′ S/55°23′ E, September 2013–February 2015). The data series from these campaigns are plotted in Fig. 1. At Sodankylä and Bern only zonal wind was measured, whereas the observations from Provence and La Réunion comprise both zonal and meridional components. The gray areas in Fig. 1 correspond to data points judged untrustworthy (measurement response < 0.8, altitude resolution > 20 km or altitude accuracy > 4 km, see Rüfenacht et al., 2014, for details). The sensitive altitude range largely depends on the signal-to-noise ratio of the receiver, which was significantly improved by an instrumental upgrade in autumn 2012. Moreover the strength of the radiation signal reaching the receiver depends on tropospheric conditions. While ice clouds are fully transparent to microwave radiation near 142 GHz, attenuation by liquid and gaseous water can negatively impact the signal-to-noise ratio, although observations remain possible even in the presence of non-precipitating liquid water clouds or fog.

2.2 ECMWF model data

The European Centre for Medium-Range Weather Forecasts (ECMWF) is a major service provider of weather and climate data products. The Operational Analysis used in this study combines meteorological data from a variety of different observing platforms with a continually updated general circulation model. The observations assimilated in a 4-D-Var assimilations window of 12 h mainly originate from the troposphere and lower stratosphere (e.g. Dee et al., 2011; ECMWF, 2016). The few observations assimilated at higher altitudes mainly originate from infrared radiation soundings (Engelen and Bauer, 2014; Dragani and McNally, 2013, and references therein). Operational Analysis is preferred over the re-analysis, i.e. ERA-Interim, principally because of the higher model top (0.01 hPa compared to 0.1 hPa). For the research presented here data from model versions 36r2 (September to November 2010), 36r4 (November 2010 to May 2011), 37r2 (May to November 2011), 37r3 (November 2011 to June 2012), 38r1 (June 2012 to June 2013), 38r2 (June to November 2013) and 40r1 (November 2013 to February 2015) with a spectral resolution of T1279 have been used (ECMWF, 2015). The analog of Fig. 1 for the ECMWF data used in the present study is given in Fig. S2 of the Supplement. A previous study revealed agreement within the measurement error between ECMWF's Operational Analysis and WIRA's wind measurements in the stratosphere, but demonstrated that the mesospheric zonal wind speed is generally significantly larger in the model for mid and high latitude stations (Rüfenacht et al., 2014). In contrast, comparisons between a limited data set of WIRA and the MERRA re-analysis from NASA's

GEOS-5 model (Rienecker et al., 2011) revealed good agreement also in the mesosphere (Le Pichon et al., 2015).

3 Data analysis

It is known from earlier research that atmospheric waves with periods ranging from 5–50 days are intermittent, showing little phase preference (e.g. Araújo et al., 2014; Day et al., 2012). Therefore we perform the spectral analyses in sliding Hamming windows encompassing three oscillation periods T. The window width matching an integer multiple of the searched period and the use of a Hamming windowing function help to minimize spectral leakage. Data gaps in the measured time series can be large at some times and altitudes, therefore gaps were not interpolated as done in other studies, because this would artificially alter the oscillation signal (damping it in case of linear interpolation). They were rather treated as missing values and the Lomb–Scargle spectral approach for irregularly spaced data was applied (Press et al., 2001; Scargle, 1982; Lomb, 1976).

The spectral method used in the present study will be described in some more details in the following: For each altitude level a wind time series $\boldsymbol{x}$ is sampled at equally spaced times $t_j = k \cdot \delta t$ with $x_j = \boldsymbol{x}(t_j)$ and $k \in \mathbb{N}$. However, for some t_j no reliable measurement data x_j exist at the respective altitude. Such pairs of (t_j, x_j) will be excluded from the following analysis leading to an unequally spaced time series. We define $\bar{x}_j$ and σ_j as the mean and standard deviation of $\boldsymbol{x}$ in the index range $(j-n)\dots(j+n)$, i.e. within a window of length $(2n+1) \approx 3T/\delta t$. The Lomb–Scargle transform $\mathcal{L}$ is applied to the windowed time series to obtain a normalized periodogram P_j for each point in time:

$$P_j = \mathcal{L}_{i \in \mathcal{B}_j}\{\, t_{j+i}\,,\, h_i \cdot (x_{j+i} - \bar{x}_j\,)\} \tag{1}$$

with the indices i in the range

$$\mathcal{B}_j = \{\, m \,|\, m \in \{\,-n, -n+1, \dots, 0, \dots, n\} \wedge \exists x_{j+m}\,\} \tag{2}$$

and with h_i being the coefficient of a Hamming window of length $(2n+1)$ centered around index 0. Let us also define:

$$\mathcal{C}_j = \{m \,|\, m \in \mathcal{B}_j \wedge |m| \cdot \delta t \leq T/2\}, \tag{3}$$

i.e. $\mathcal{C}_j$ denotes the central third of $\mathcal{B}_j$. P_j's calculated from windows with an insufficient amount of relevant data points, i.e. when

$$\#\mathcal{B}_j < \frac{T}{\delta t} \quad \vee \quad \#\mathcal{C}_j < \frac{T}{3\delta t} \tag{4}$$

are rejected from the analysis. The entire procedure is repeated for all searched oscillation periods T, for all times t_j and for all altitude levels. In Eqs. (2) to (4) $\wedge$ and $\vee$ denote logical "and" and "or" while the cardinality operator $\#$ returns the number of elements of its argument.

The normalized periodogram P_j is readily transformed to the amplitude spectrum (e.g. by combining Eq. 6 from Hocke, 1998, and Eq. 15 from Harris, 1978):

$$A_j(T) = 2\sigma_j \sqrt{\frac{\sum_{i \in \mathcal{B}_j} h_i^2}{\left(\sum_{i \in \mathcal{B}_j} h_i\right)^2} P_j(T)}. \tag{5}$$

P_j also contains the information about the significance α of an oscillation peak at a distinct frequency

$$\alpha_j(T) = 1 - [1 - \exp(-P_j(T))]^M . \tag{6}$$

In our case M is a factor close to the window width (for details see Press et al., 2001). The variable α might also be referred to as "false alarm probability of the detection", a small α value indicates a highly significant oscillation.

For comparison, the pseudo-wavelet approach used by Studer et al. (2012) and Scheiben et al. (2014) has been modified in order not to rely on interpolation. The difference between the results obtained with the modified pseudo-wavelet method shown in Figs. ~~S2 and~~ S3 and S4 in the Supplement and the outcomes of the Lomb–Scargle method (Figs. 2 and 5) was found to be small. Moreover, the different spectral methods with and without interpolation and with different windowing functions have been tested for their ability of retrieving synthetic oscillation signals containing data gaps correctly. The Lomb–Scargle method used with a Hamming window applied in the analyses presented in this paper was most successful and produced only marginal differences between the retrieved and the initial signal, but the pseudo-wavelet approach without interpolation of the data gaps used for Figs. ~~S2 and~~ S3 and S4 also provided satisfying results.

4 Results

Spectral analyses have been performed on daily average wind profiles by WIRA and ECMWF Operational Analysis. In order to allow direct comparisons between measurements and model, the ECMWF data were convolved with WIRA's averaging kernels to account for the limited vertical resolution of the radiometer and data gaps were added at the times t_j where the measurement did not provide reliable data. In the following, the model data treated in this way are referred to as “ECMWF at WIRA”.

4.1 Altitude dependence of the periodograms

The altitude dependent temporally averaged periodograms of the horizontal wind measurements by WIRA are shown in Fig. 2. The temporal average runs over all oscillation amplitude data existing at a certain altitude for the respective campaign. From Fig. 1 one can identify levels where trustworthy measurement data are predominantly present during winter, because the generally wetter summer troposphere alters the signal-to-noise ratio of the observation setup as a consequence of a stronger attenuation of the middle-atmospheric radiation. At these altitudes the oscillation amplitudes should thus not be interpreted as averages over the entire duration of the campaign. This is especially the case for the upper altitude data from Sodankylä (above approx. 0.2 hPa) but to a lesser extent also applies to the other stations.

Figure 2 indicates that the dominant oscillations in horizontal wind occur in the extra-long period range (20–50 days) at all stations. Atmospheric oscillations with periods around 27 days are often discussed in the context of the modulation of the solar forcing with the rotational period of the sun (e.g. Fedulina et al., 2004; Huang et al., 2015). However, cross-correlation analyses of WIRA's wind measurements with solar UV irradiance data revealed that the phase difference between wind and irradiance time series varies significantly for the different measurement campaigns. From this fact and from the obvious seasonality (see Sect. 4.2) of these wind oscillations observed during the maximum phase of solar cycle 24 we infer that the influences of the variations in the solar forcing on middle atmospheric horizontal winds must be indirect, if existing. Similar conclusions were drawn by a study with the WACCM model to be presented in a separate publication where it is demonstrated that periods around 27 days can also be produced inherently by the atmosphere and that oscillations in the solar irradiance can manifest themselves in the atmospheric wind periodograms at frequencies differing from the variations in solar forcing (Ansgar Schanz, personal communication, 2015). Huang et al. (2015) indicate that their observed extra-long period oscillation might be an atmospheric normal mode and that it may be indirectly introduced by the modulation of tropospheric convective activity with the solar rotation period. Fedulina et al. (2004) report a modulation of the 5-day wave amplitude with a period of 25 to 35 days but point out that a correlation with solar activity might appear by coincidence regarding the considered time scales.

Normal modes in the atmosphere are known to have oscillation periods around 2, 5, 10 and 16 days (Salby, 1981a, b) which can also be observed in the average periodograms of WIRA measurements for the different campaigns. According to the Nyquist theorem, measurements of daily average wind profiles do not allow to draw meaningful conclusions regarding the behavior of the quasi 2-day periodicity. A quasi 5-day wave is observed in WIRA's zonal wind measurements for Bern and Sodankylä, and for the zonal and meridional winds on La Réunion. The 5-day signal in the meridional wind in Provence has lower significance and seems to be an artifact of the measurement situation as it is also present in Fig. 3 showing “ECMWF at WIRA” data but not in the periodogram of the unaltered ECMWF data in Fig. 4. It might originate from the small data gap at the beginning of January 2013 (see Figs. 5 and 6) at a time of high variability due to a major sudden stratospheric warming. Oscillations with periods around 10 days are clearly visible in the zonal wind in Sodankylä and the zonal and meridional wind in Provence. A quasi 16-day variation is weakly recognizable in the zonal wind measurements from La Réunion.

High interannual variability has to be expected (e.g. compare the results from the Bern and the Provence campaign which were sampled at very close geographical locations). Despite this variability, one might conclude from the WIRA data that zonal wind oscillations tend to be strongest at mid latitudes, and that meridional wind oscillations are weaker in the tropics than at mid-latitudes. This hypothesis is supported by Figs. ~~S4 to S7~~ S5 to S8 showing ECMWF data for more extended time intervals at the campaign sites. It also confirms previous studies based on observations or assimilated model data (Hirota and Hirooka, 1984; Hirooka and Hirota, 1985; Day et al., 2011; Fedulina et al., 2004). The highest oscillation amplitudes are usually detected around the stratopause which is also the region where the highest absolute wind speeds are generally observed (e.g. Rüfenacht et al., 2014). The reduced wave activity in the mesosphere, particularly above 0.1 hPa, may be explained by planetary wave breaking in the stratosphere (e.g. McIntyre and Palmer, 1983; Brasseur and Solomon, 2005). Interestingly this consideration also applies to the extra-long period oscillations what is in line with the periodograms of geopotential heights from MLS at mid-latitudes presented by Studer et al. (2012). In the interpretation of Fig. 2 we should keep in mind that the limited vertical resolution of WIRA, which is around 12 km (i.e. 0.75 pressure decades) at these altitudes, may vertically smear out the oscillation peaks.

The only major exception to the quiet mesosphere in Fig. 2 is the 27-day peak around 0.1 hPa in the periodogram for Sodankylä. This oscillation can probably be regarded as a special case as it occurs in the vicinity of the major sudden stratospheric warming event of January 2012 as seen from supplementary Fig. ~~S12~~ S13 which displays the oscillation activity at 0.05 hPa. Although based on very few data points, the slight increase near the

16-day periodicity at the very top of the retrieval range might be understood as an influence of the strengthening of this signal in the MLT region reported by other observational studies (e.g. Williams and Avery, 1992; Day et al., 2012).

The analysis for the scenario ECMWF at WIRA shown in Fig. 3 should yield identical results as presented in Fig. 2 if the ~~measruements~~ measurements are error-free and the atmosphere is realistically represented by the model. In this case WIRA and ECMWF would agree that the periodograms of the real atmosphere correspond to Fig. 4. The qualitative and quantitative agreement between measurements and model is remarkably good below 0.3 hPa. The only notable discrepancies occur at periods larger than 45 days, for the 5-day wave which is mostly absent in ECMWF and for the 10-day periodicity. The last one is present in ECMWF with amplitudes comparable to WIRA only for the meridional wind during the Provence campaign.

Above 0.3 hPa ECMWF tends to produce higher oscillation amplitudes than WIRA. Wind oscillation amplitudes observed in the MLT region (e.g. Araújo et al., 2014; Luo et al., 2001, 2002) better match with the uppermost observations from WIRA than with the high amplitudes in the ECMWF model.

A previous study (Rüfenacht et al., 2014) has shown that, in comparison with WIRA, ECMWF generally features stronger mesospheric zonal winds with discrepancies increasing for higher altitudes. When normalizing the oscillation amplitudes by dividing by the mean wind profile of the measurement campaign at the respective altitude the differences between WIRA and ECMWF were highly diminished (Fig. S13 in the Supplement). This shows that the oscillation amplitude discrepancy behaves similarly to the absolute wind speed discrepancy, i.e. increases by the same factor with increasing altitude. Knowing that the ECMWF model is constrained by the assimilation of tropospheric and stratospheric data but is mainly free-running in the mesosphere (Orr et al., 2010; ECMWF, 2016), one might conclude that some of ECMWF's model physics are not accurate enough to reproduce the dynamics of the mesosphere ~~to~~ in detail. An overestimation of the upward ~~momentum transport~~ transport of horizontal momentum or an underestimation of some damping mechanisms in the mesosphere are possible causes of this effect. Another explanation might be that the model contains assumptions on the balance between the wind and temperature fields which are not accurate in the mesosphere. As noted by Shepherd et al. (2000) and Koshyk et al. (1999) the unbalanced component of the flow increases with altitude. However, the exact reason for the concomitant mesospheric discrepancies between ECMWF's and WIRA's absolute wind speeds and oscillation amplitudes remain unclear.

4.2 Temporal evolution of the periodograms

Atmospheric waves and oscillations can be intermittent in nature (i.e. wave-packets) and~~seasonality might be present~~/or seasonally constrained. Accordingly, the temporal evolution of the oscillations was examined. Figures 5, 6 and 7 display the results for WIRA, ECMWF at WIRA and unaltered ECMWF data, respectively, at stratopause level where the highest amplitudes have generally been observed. Contours indicating the significance levels of the oscillation peaks according to Eq. (6) are overlaid to the amplitude plots. Again, Fig. 7 would show the behavior of the real atmosphere represented by the measurements of WIRA in case Figs. 5 and 6 exactly match.

From the analyses it becomes obvious that the dominant oscillation in the extra-long period range is always highly significant. The oscillation peaks for ECMWF data are slightly more significant what is consistent with the absence of measurement noise.

A clear seasonality is apparent for all observations and model data with oscillation activities being much stronger in the winter half year for all oscillation periods covered by the present study. The seasonality is also visible for other years at the campaign sites as shown by ECMWF data (Figs. ~~S8 to S11~~ S9 to S12 of the Supplement) and is in accordance with other observational studies of stratopause level oscillations (Hirooka and Hirota, 1985; Day et al., 2011; Studer et al., 2012) and especially with the climatological periodogram of zonal wind at 58 km in Fig. 5 of Luo et al. (2001). As in the mentioned climatology, no quasi 5-day wave signature could be found in the summer data from WIRA, in contrast to the results of Hirota and Hirooka (1984) and Fedulina et al. (2004) which indicate the frequent presence of such a wave at the summer stratopause.

The same pattern of seasonality as for the high and mid latitude stations is observed on La Réunion although it is located in the southern tropics (21°04′ S). One can infer that the station is substantially influenced by mid-latitude dynamics. This influence is also recognizable in the time series of the observed zonal wind (Fig. 1) where the mid-latitudinal annual variation mostly dominates over tropical semi-annual variation, although the latter one is still clearly visible.

During WIRA's measurement campaigns in the ~~northern hemisphere~~ Northern Hemisphere two major sudden stratospheric warmings occurred in mid January 2012 and at the beginning of January 2013. Previous studies (e.g. Alexander and Shepherd, 2010; Day et al., 2011; Scheiben et al., 2014) reported a strong decrease in planetary wave activity in the days and weeks following the onset of major warmings. This feature can nicely be seen in WIRA and ECMWF data for the Provence campaign, but the effect is absent from both data sets for the Sodankylä campaign.

The period of the extra-long period oscillations is not constant between the different campaigns. It can even vary within a single occurrence of the oscillation as seen in the example of Bern where the period decreases from 35 to 25 days between December 2010 and March 2011. A 10 days period change is at the limit of the spectral resolution of our analysis method for this long periodicities. Nevertheless it may be interpreted as a real signal, not only due to the monotony of the decrease, but also to an additional check using our spectral method with rectangular instead of Hamming windowing in order to improve the spectral resolution (not shown). A similar feature has simultaneously been observed at three different sites from high to lower mid-latitudes in the mesopause region by Luo et al. (2001). This study also noted that the extra-long period oscillation often appears in combination with a quasi 16-day wave. The occurrence of this periodicity has not been obvious from Figs. 2 and 3 because it had been masked by other oscillation signals in the temporal average. In contrast, it is clearly identifiable as independent periodicity in Figs. 5 and 6. In the Bern and the La Réunion time series the strongest 16-day amplitudes (lasting for about 1 period) are observed near the initiation and the termination of the persistent extra-long period oscillation with a duration of 80 and 50 days, respectively. The duration of the presence of these oscillations is comparable to the results for mesopause wind presented by Luo et al. (2001). However, it should be noted that if the extra-long period oscillation is abruptly initiated or terminated, the 16-day signal could be produced as an artifact of the used spectral method as simulations showed. Whether a real 16-day wave is present and whether the two oscillations are linked in some way will have to be verified in further studies.

In general the agreement between WIRA and ECMWF at stratopause level is very good in terms of timing, amplitude and frequency. The extra-long oscillations in zonal wind at the two mid latitude stations of Bern and Provence are slightly stronger in the WIRA time series and the amplitude of the quasi 16-day wave in the zonal wind is slightly enhanced for the measurements. However, the most notable difference between WIRA and ECMWF appears at shorter periods. Although mostly not statistically significant, ECMWF seems to underestimate variablities with periods shorter than 10 days for all measurement campaigns. A similar feature has been found for the comparison of middle-atmospheric temperature lidar observations from Observatoire de Haute Provence and Table Mountain (34°24′ N, 117°42′ W) with ECMWF model data (Le Pichon et al., 2015).

5 Conclusions

Long and extra-long period oscillations in the horizontal wind have been observed by the novel ground-based Doppler wind radiometer WIRA in the altitude range between mid-stratosphere (5 hPa) and upper mesosphere (0.02 hPa) at low, mid and high latitudes. In this altitude range wind observations are extremely sparse and the measurement time series from WIRA are the only ones satisfying the necessary conditions for the study of this type of oscillations.

The dominant oscillations were found to lie in the extra-long period band (20–50 days) with the features showing pronounced temporal intermittency and the period being subject to temporal variations. A direct link between the solar forcing and these atmospheric periodicities could not be established, however solar forcing might influence the atmospheric wave pattern in an indirect way. Enhanced quasi 16-day oscillation activity has sometimes been detected in the vicinity of strong extra-long period oscillations. A more extended study would however be needed to establish the origin of this signal and to uncover a potential link between the quasi 16-day wave and the extra-long periodicities. In addition to the extra-long period oscillations, normal modes with periods near 5, 10 and 16 days are present in our observations. All observed oscillations manifest a strong seasonality with amplitudes being much higher during the winter half year. The strongest oscillation amplitudes were usually found around the stratopause.

WIRA observations and ECMWF model data agree remarkably well below 0.3 hPa. At higher altitudes ECMWF features higher oscillation amplitudes than the observations, a discrepancy behaving similarly to what has been noted for the discrepancy in absolute wind speeds in a previous study. In addition, ECMWF Operational Analysis data shows reduced variability at periods below 10 days as compared with the measurements by WIRA. More detailed validations of numerical weather prediction models such as ECMWF in the middle-atmosphere will be an important task for the near future and shall among others be addressed in the framework of the ARISE project (Blanc et al., 2015). Wind radiometer data could provide a valuable contribution to such research.

Data availability

We acknowledge ECMWF for the Operational Analysis data (www.ecmwf.int) as well as NASA for the Aura MLS temperature profiles (http://disc.gsfc.nasa.gov/acdisc) used in WIRA's retrieval algorithm in the way described in Rüfenacht et al. (2014). The WIRA data presented in this manuscript can be made available on request.

The Supplement related to this article is available online at doi:10.5194/acpd-0-1-2016-supplement.

Acknowledgements. This work has been supported by the Swiss National Science Foundation grants number 200020–146388 and 200020–160048. We especially thank the staff of the Observatoire du Maïdo, of the Observatoire de Haute-Provence and of the Finnish Meteorological Institute in Sodankylä for the hospitality and support during the measurement campaigns.

References

Alexander, S. P. and Shepherd, M. G.: Planetary wave activity in the polar lower stratosphere, Atmos. Chem. Phys., 10, 707–718, doi:10.5194/acp-10-707-2010, 2010.

Allan, D.: Statistics of atomic frequency standards, P. IEEE, 54, 221–230, doi:10.1109/PROC.1966.4634, 1966.

Araújo, L. R., Lima, L. M., Batista, P. P., Clemesha, B. R., and Takahashi, H.: Planetary wave seasonality from meteor wind measurements at 7.4° S and 22.7° S, Ann. Geophys., 32, 519–531, doi:10.5194/angeo-32-519-2014, 2014.

Baldwin, M. P., Stephenson, D. B., Thompson, D. W. J., Dunkerton, T. J., Charlton, A. J., and O'Neill, A.: Stratospheric memory and skill of extended-range weather forecasts, Science, 301, 636–640, doi:10.1126/science.1087143, 2003a.

Baldwin, M. P., Thompson, D. W. J., Shuckburgh, E. F., Norton, W. A., and Gillett, N. P.: Weather from the stratosphere?, Science, 301, 317–319, doi:10.1126/science.1085688, 2003b.

Baumgarten, G.: Doppler Rayleigh/Mie/Raman lidar for wind and temperature measurements in the middle atmosphere up to 80 km, Atmos. Meas. Tech., 3, 1509–1518, doi:10.5194/amt-3-1509-2010, 2010.

Blanc, E., Charlton-Perez, A., Keckhut, P., Evers, L., Heinrich, P., Le Pichon, A., and Hauchecorne, A.: The ARISE project: dynamics of the atmosphere and climat, Our Common Future Under Climate Change, International Scientific Coference, https://hal-insu.archives-ouvertes.fr/insu-01183228, poster, 2015.

Brasseur, B. H. and Solomon, S.: Aeronomy of the Middle Atmosphere, Springer, 3rd edn., 2005.

Charlton, A. J., O'Neill, A., Lahoz, W. A., and Massacand, A. C.: Sensitivity of tropospheric forecasts to stratospheric initial conditions, Q. J. Roy. Meteor. Soc., 130, 1771–1792, doi:10.1256/qj.03.167, 2004.

Day, K. A., Hibbins, R. E., and Mitchell, N. J.: Aura MLS observations of the westward-propagating s=1, 16-day planetary wave in the stratosphere, mesosphere and lower thermosphere, Atmos. Chem. Phys., 11, 4149–4161, doi:10.5194/acp-11-4149-2011, 2011.

Day, K. A., Taylor, M. J., and Mitchell, N. J.: Mean winds, temperatures and the 16- and 5-day planetary waves in the mesosphere and lower thermosphere over Bear Lake Observatory (42° N, 111° W), Atmos. Chem. Phys., 12, 1571–1585, doi:10.5194/acp-12-1571-2012, 2012.

Dee, D. P., Uppala, S. M., Simmons, A. J., Berrisford, P., Poli, P., Kobayashi, S., Andrae, U., Balmaseda, M. A., Balsamo, G., Bauer, P., Bechtold, P., Beljaars, A. C. M., van de Berg, L., Bidlot, J., Bormann, N., Delsol, C., Dragani, R., Fuentes, M., Geer, A. J., Haimberger, L., Healy, S. B., Hersbach, H., Hólm, E. V., Isaksen, L., Kållberg, P., Köhler, M., Matricardi, M., McNally, A. P., Monge-Sanz, B. M., Morcrette, J.-J., Park, B.-K., Peubey, C., de Rosnay, P., Tavolato, C., Thépaut, J.-N., and Vitart, F.: The ERA-Interim reanalysis: configuration and performance of the data assimilation system, Q. J. Roy. Meteor. Soc., 137, 553–597, doi:10.1002/qj.828, 2011.

Dragani, R. and McNally, A. P.: Operational assimilation of ozone-sensitive infrared radiances at ECMWF, Q. J. R. Meteorol. Soc., 139, 2068–2080, doi:10.1002/qj.2106, 2013.

ECMWF: available at: http://www.ecmwf.int/en/forecasts/documentation-and-support/changes-ecmwf-model, last access: 15 June 2015.

ECMWF: https://software.ecmwf.int/wiki/display/IFS/Official+IFS+Documentation, accessed 15 Feb 2016, 2016.

Engelen, R. J. and Bauer, P.: The use of variable CO_2 in the data assimilation of AIRS and IASI radiances, Q. J. R. Meteorol. Soc., 140, 958–965, doi:10.1002/qj.919, 2014.

Eriksson, P., Jimenez, C., and Buehler, S.: Qpack, a general tool for instrument simulation and retrieval work, J. Quant. Spectrosc. Ra., 91, 47–64, doi:10.1016/j.jqsrt.2004.05.050, 2005.

Eriksson, P., Buehler, S., Davis, C., Emde, C., and Lemke, O.: ARTS, the atmospheric radiative transfer simulator, version 2, J. Quant. Spectrosc. Ra., 112, 1551–1558, doi:10.1016/j.jqsrt.2011.03.001, 2011.

Fedulina, I. N., Pogoreltsev, A. I., and Vaughan, G.: Seasonal, interannual and short-term variability of planetary waves in Met Office stratospheric assimilated fields, Q. J. R. Meteorol. Soc., 130, 2445–2458, doi:10.1256/qj.02.200, 2004.

Guharay, A., Batista, P., Clemesha, B., and Buriti, R.: Observations of the intraseasonal oscillations over two Brazilian low latitude stations: a comparative study , J. Atmos. Sol.-Terr. Phy., 120, 62–69, doi:10.1016/j.jastp.2014.08.016, 2014.

Hardiman, S. C., Butchart, N., Charlton-Perez, A. J., Shaw, T. A., Akiyoshi, H., Baumgaertner, A., Bekki, S., Braesicke, P., Chipperfield, M., Dameris, M., Garcia, R. R., Michou, M., Pawson, S., Rozanov, E., and Shibata, K.: Improved predictability of the troposphere using stratospheric final warmings, J. Geophys. Res.-Atmos., 116, D18113, doi:10.1029/2011JD015914, 2011.

Harris, F. J.: On the use of windows for harmonic analysis with the discrete Fourier transform, P. IEEE, 66, 51–83, doi:10.1109/PROC.1978.10837, 1978.

Hildebrand, J., Baumgarten, G., Fiedler, J., Hoppe, U.-P., Kaifler, B., Lübken, F.-J., and Williams, B. P.: Combined wind measurements by two different lidar instruments in the Arctic middle atmosphere, Atmos. Meas. Tech., 5, 2433–2445, doi:10.5194/amt-5-2433-2012, 2012.

Hirooka, T. and Hirota, I.: Normal Mode Rossby Waves Observed in the Upper Stratosphere. Part II: Second Antisymmetric and Symmetric Modes of Zonal Wavenumbers 1 and 2, J. Atmos. Sci., 42, 536–548, doi:10.1175/1520-0469(1985)042<0536:NMRWOI>2.0.CO;2, 1985.

Hirota, I. and Hirooka, T.: Normal Mode Rossby Waves Observed in the Upper Stratosphere. Part I: First Symmetric Modes of Zonal Wavenumbers 1 and 2, J. Atmos. Sci., 41, 1253–1267, doi:10.1175/1520-0469(1984)041<1253:NMRWOI>2.0.CO;2, 1984.

Hocke, K.: Phase estimation with the Lomb–Scargle periodogram method, Ann. Geophys., 16, 356–358, 1998.

Hocke, K., Studer, S., Martius, O., Scheiben, D., and Kämpfer, N.: A 20-day period standing oscillation in the northern winter stratosphere, Ann. Geophys., 31, 755–764, doi:10.5194/angeo-31-755-2013, 2013.

Huang, K. M., Liu, A. Z., Zhang, S. D., Yi, F., Huang, C. M., Gan, Q., Gong, Y., Zhang, Y. H., and Wang, R.: Observational evidence of quasi-27-day oscillation propagating from the lower atmosphere to the mesosphere over 20° N, Ann. Geophys., 33, 1321–1330, doi:10.5194/angeo-33-1321-2015, 2015.

Keckhut, P.: Mid-latitude summer response of the middle atmosphere to short-term solar UV changes, Ann. Geophys., 13, 641–647, doi:10.1007/s00585-995-0641-7, 1995.

Koshyk, J. N., Boville, B. A., Hamilton, K., Manzini, E., and Shibata, K.: Kinetic energy spectrum of horizontal motions in middle-atmosphere models, J. Geophys. Res.-Atmos., 104, 27177–27190, doi:10.1029/1999JD900814, 1999.

Le Pichon, A., Assink, J. D., Heinrich, P., Blanc, E., Charlton-Perez, A., Lee, C. F., Keckhut, P., Hauchecorne, A., Rüfenacht, R., Kämpfer, N., Drob, D. P., Smets, P. S. M., Evers, L. G., Ceranna, L., Pilger, C., Ross, O., and Claud, C.: Comparison of co-located independent ground-based middle-atmospheric wind and temperature measurements with numerical weather prediction models, J. Geophys. Res.-Atmos., 120, 8318–8331, doi:10.1002/2015JD023273, 2015.

Lomb, N. R.: Least-squares frequency analysis of unequally spaced data, Astrophys. Space Sci., 39, 447–462, doi:10.1007/BF00648343, 1976.

Luo, Y., Manson, A. H., Meek, C. E., Thayaparan, T., MacDougall, J., and Hocking, W. K.: Extra long period (20–40 day) oscillations in the mesospheric and lower thermospheric winds: observations in Canada, Europe and Japan, and considerations of possible solar influences, J. Atmos. Sol.-Terr. Phy., 63, 835–852, doi:10.1016/S1364-6826(00)00206-6, 2001.

Luo, Y., Manson, A. H., Meek, C. E., Thayaparan, T., MacDougall, J., and Hocking, W. K.: The 16-day wave in the mesosphere and lower thermosphere: simultaneous observations at Saskatoon (52° N, 107° W) and London (43° N, 81° W), Canada, J. Atmos. Sol.-Terr. Phy., 64, 1287–1307, doi:10.1016/S1364-6826(02)00042-1, 2002.

McIntyre, M. E. and Palmer, T. N.: Breaking planetary waves in the stratosphere, Nature, 305, 593–600, doi:10.1038/305593a0, 1983.

Müllemann, A. and Lübken, F.-J.: Horizontal winds in the mesosphere at high latitudes, coupling processes in the MLT region, Adv. Space Res., 35, 1890–1894, doi:10.1016/j.asr.2004.11.014, 2005.

National Research Council: United States Space Science Program: Report to COSPAR, Ninth Meeting, National Academy of Sciences, 1966.

Orr, A., Bechtold, P., Scinocca, J., Ern, M., and Janiskova, M.: Improved middle atmosphere climate and forecasts in the ECMWF model through a nonorographic gravity wave drag parameterization, J. Climate, 23, 5905–5926, doi:10.1175/2010JCLI3490.1, 2010.

Press, W. H., Teukolsky, S. A., Vetterling, W. T., and Flannery, B. P.: Numerical Recipes in Fortran 77: The Art of Scientific Computing, 2nd edn., Cambridge University Press, New York, NY, USA, 2001.

Rienecker, M. M., Suarez, M. J., Gelaro, R., Todling, R., Bacmeister, J., Liu, E., Bosilovich, M. G., Schubert, S. D., Takacs, L., Kim, G.-K., Bloom, S., Chen, J., Collins, D., Conaty, A., da Silva, A., Gu, W., Joiner, J., Koster, R. D., Lucchesi, R., Molod, A., Owens, T., Pawson, S., Pegion, P., Redder, C. R., Reichle, R., Robertson, F. R., Ruddick, A. G., Sienkiewicz, M., and Woollen, J.: MERRA: NASA's Modern-Era Retrospective Analysis for Research and Applications, J. Climate, 24, 3624–3648, doi:10.1175/JCLI-D-11-00015.1, 2011.

Rodgers, C. D.: Inverse Methods for Atmospheric Sounding: Theory and Practice, Vol. 2 of Series on Atmospheric, Oceanic and Planetary Physics, World Scientific, Singapore, reprint 2008, 2000.

Rüfenacht, R., Kämpfer, N., and Murk, A.: First middle-atmospheric zonal wind profile measurements with a new ground-based microwave Doppler-spectro-radiometer, Atmos. Meas. Tech., 5, 2647–2659, doi:10.5194/amt-5-2647-2012, 2012.

Rüfenacht, R., Murk, A., Kämpfer, N., Eriksson, P., and Buehler, S. A.: Middle-atmospheric zonal and meridional wind profiles from polar, tropical and midlatitudes with the ground-based microwave Doppler wind radiometer WIRA, Atmos. Meas. Tech., 7, 4491–4505, doi:10.5194/amt-7-4491-2014, 2014.

Salby, M. L.: Rossby normal modes in nonuniform background configurations. Part I: Simple fields, J. Atmos. Sci., 38, 1803–1826, doi:10.1175/1520-0469(1981)038<1803:RNMINB>2.0.CO;2, 1981a.

Salby, M. L.: Rossby normal modes in nonuniform background configurations. Part II. Equinox and solstice conditions, J. Atmos. Sci., 38, 1827–1840, doi:10.1175/1520-0469(1981)038<1827:RNMINB>2.0.CO;2, 1981b.

Scargle, J. D.: Studies in astronomical time-series analysis. II. Statistical aspects of spectral-analysis of unevenly spaced data, Astrophys, J., 263, 835–853, doi:10.1086/160554, 1982.

Scheiben, D., Tschanz, B., Hocke, K., Kämpfer, N., Ka, S., and Oh, J. J.: The quasi 16-day wave in mesospheric water vapor during boreal winter 2011/2012, Atmos. Chem. Phys., 14, 6511–6522, doi:10.5194/acp-14-6511-2014, 2014.

Shepherd, T. G., Koshyk, J. N., and Ngan, K.: On the nature of large-scale mixing in the stratosphere and mesosphere, J. Geophys. Res.-Atmos., 105, 12433–12446, doi:10.1029/2000JD900133, 2000.

Sigmond, M., Scinocca, J. F., Kharin, V. V., and Shepherd, T. G.: Enhanced seasonal forecast skill following stratospheric sudden warmings, Nat. Geosci., 6, 98–102, doi:10.1038/NGEO1698, 2013.

Studer, S., Hocke, K., and Kämpfer, N.: Intraseasonal oscillations of stratospheric ozone above Switzerland, J. Atmos. Sol.-Terr. Phy., 74, 189–198, doi:10.1016/j.jastp.2011.10.020, 2012.

Williams, C. R. and Avery, S. K.: Analysis of long-period waves using the mesosphere-stratosphere-troposphere radar at Poker Flat, Alaska, J. Geophys. Res.-Atmos., 97, 20 855–20 861, doi:10.1038/305593a0, 1992.

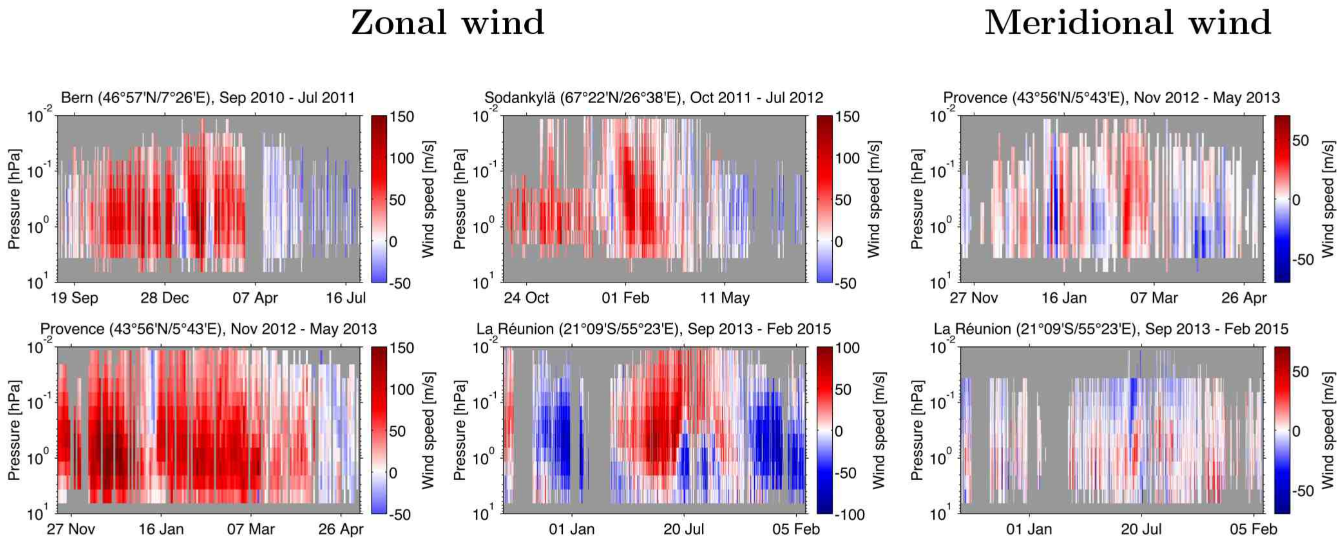

Figure 1. The zonal and meridional wind time series measured by WIRA during four different measurement campaigns analyzed in the present study. The gray areas correspond to data points judged untrustworthy according to the conditions indicated in the text. Please note the different color scale for zonal and meridional wind.

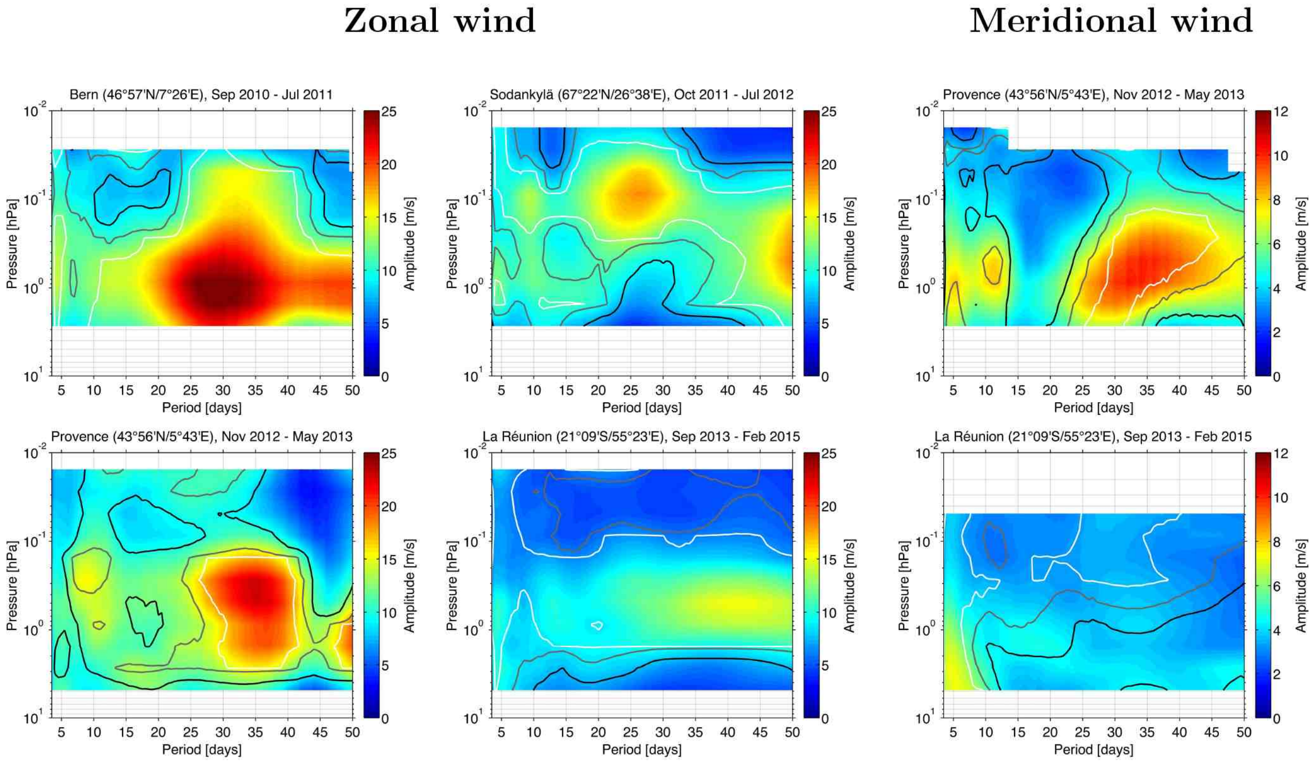

Figure 2. Temporally averaged periodograms of zonal and meridional wind profiles measured by WIRA. The black, gray and white contour lines mark $\alpha = 0.5$, 0.1 and 0.01, where the lowest value, i.e. the white contour, corresponds to the highest significance. The values of α were calculated from Eqs. (5) and (6) based on the average oscillation amplitude and the noise of the entire wind measurement time series determined using the Allan standard deviation (detrended version of the standard deviation e.g. Allan, 1966). The white areas represent altitudes and periods (i.e. window widths) for which the conditions of Eq. (4) are not satisfied, i.e. for which WIRA cannot provide reliable information due to an insufficient number of data points.

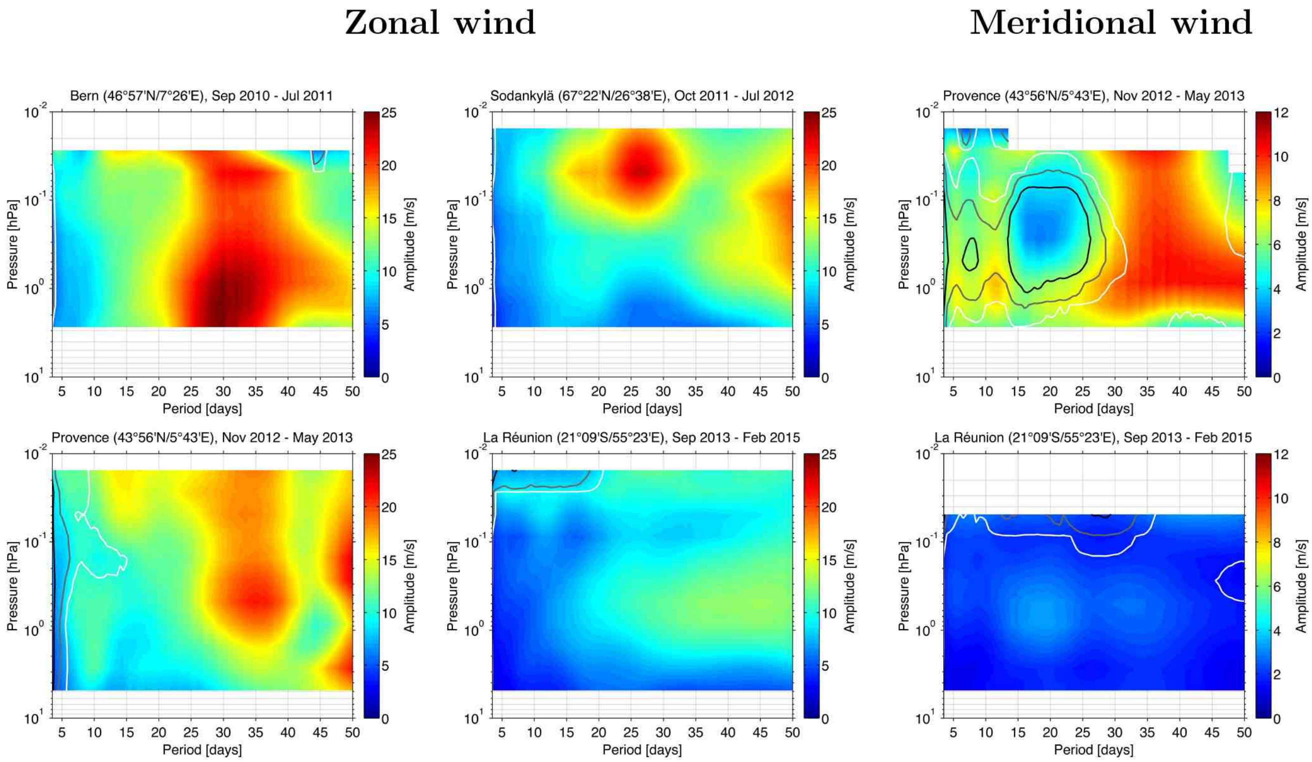

Figure 3. As Fig. 2 but for the scenario ECMWF at WIRA, i.e. for ECMWF profiles convolved with WIRA's averaging kernels and with data gaps introduced where WIRA did not provide reliable measurements.

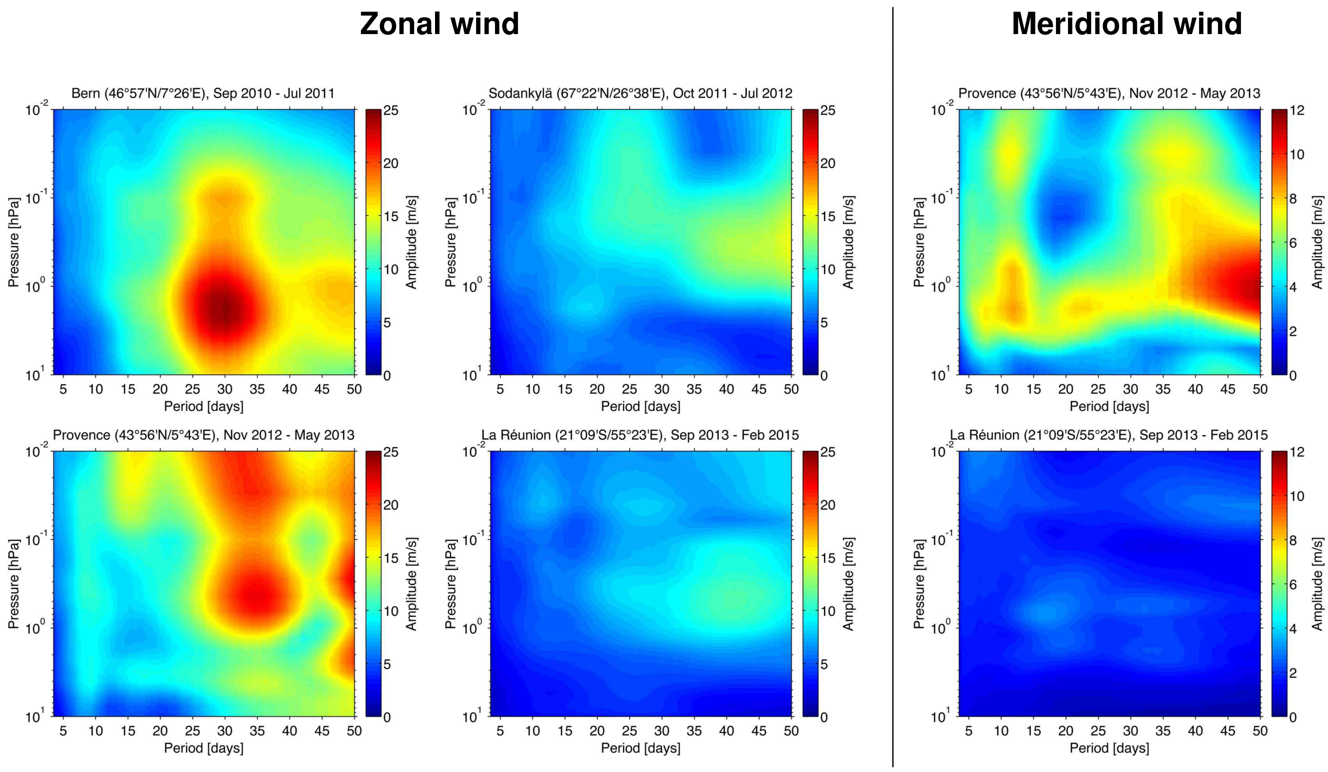

Figure 4. As Fig. 3 but for the unaltered daily average wind data from the ECMWF operational analysis.

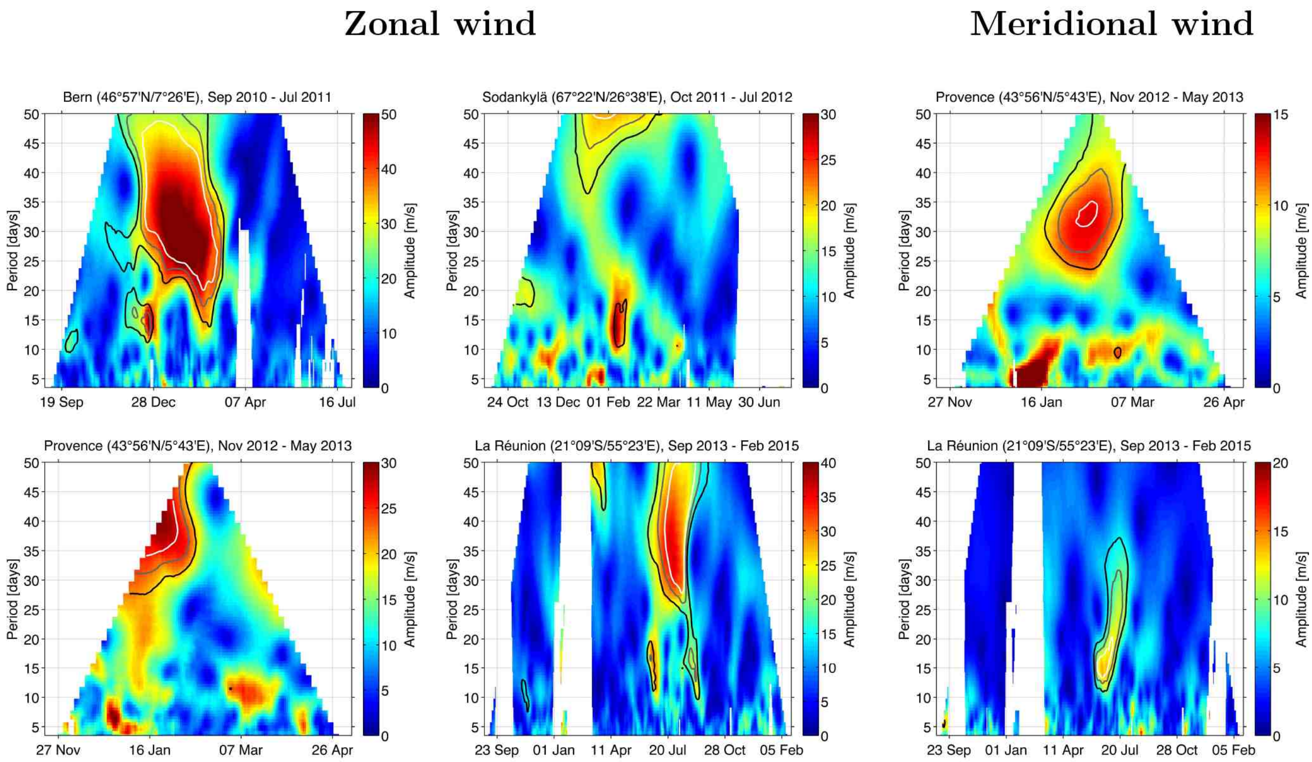

Figure 5. Temporal evolution of the periodogram at stratopause level (0.9 hPa) for wind measurements taken by WIRA. The black, gray and white contour lines mark $\alpha = 0.5$, 0.1 and 0.01 according to Eq. (6). The lowest value, i.e. the white contour, corresponds to highest significance. White areas represent times for which $\mathcal{B}_j$ contains indices before the start date of after the end date of the respective measurement campaign (what entails the trapezoidal shape of the colored area). Other areas are blanked out because the conditions of Eq. (4) are not satisfied, i.e. WIRA cannot provide reliable information due to an insufficient number of data points. Please note the occurrence of 16-day oscillations near the onset and the termination of the extra-long period oscillation in zonal wind for Bern and La Réunion.

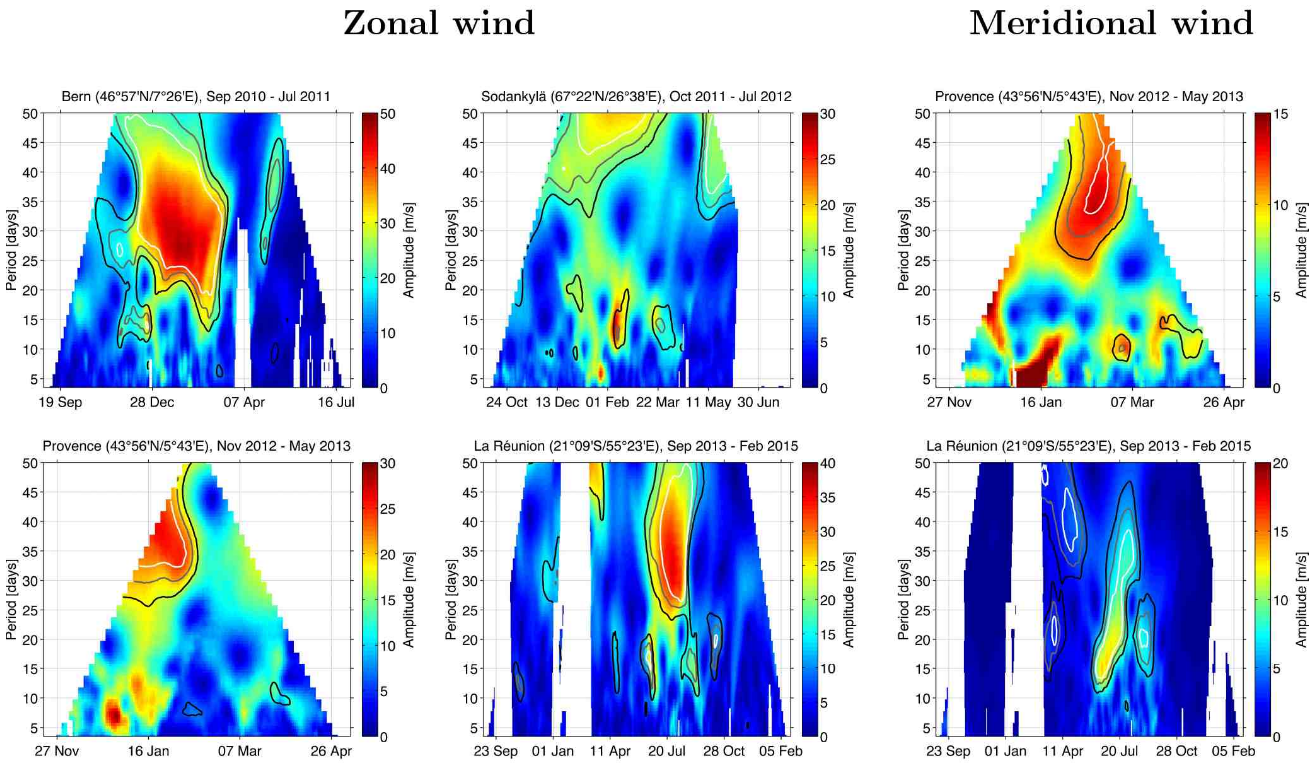

Figure 6. As Fig. 5 but for the scenario ECMWF at WIRA.

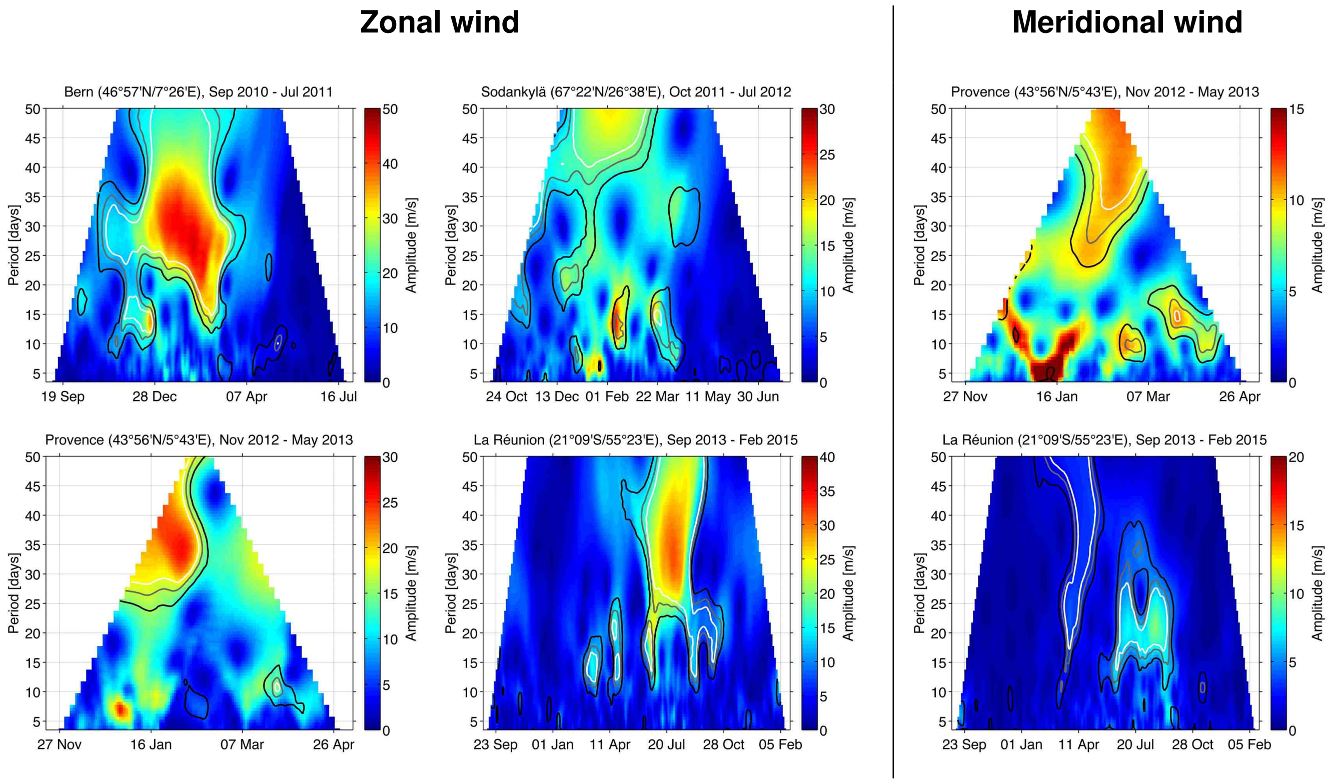

Figure 7. As Fig. 6 but for the unaltered daily average wind data from the ECMWF operational analysis.

Introduction

This Supplement provides additional figures to the main article along with descriptions of these graphics. It also contains an overview of currently available wind measurement techniques and their sensitive altitude range.

Text S1. It is interesting to note that in contrast to other atmospheric layers, observations of horizontal wind between 35 and 70 km are extremely rare as illustrated by Fig. S1. The troposphere and lower stratosphere region is covered by a number of techniques such as the widely used balloon-borne radiosondes (e.g Goldberg et al., 2004), ground-based radars (e.g. Luce et al., 2001; Hooper et al., 2008) and lidars (e.g. Gentry et al., 2000). Sodar (Sonic Detection And Ranging) observations are limited to the lowermost tropospheric altitudes (e.g. Anandan et al., 2008). After its launch planned for 2016 the space-borne lidar ADM-Aeolus will provide wind data up to 26 km on a global scale (Stoffelen et al., 2006; Elfving, 2015).

Upper-atmospheric wind measurements can be provided by ground-based and space-borne airglow or absorption interferometry of atomic or molecular oxygen and hydroxyl (Gault et al., 1996a, b; Hays et al., 1993). Currently, observations from TIDI on the TIMED satellite are available for altitudes above 70 km (Killeen et al., 2006). Previously, mesospheric observations down to 65 km and stratospheric daylight wind observations up to 40 km had been performed by HRDI on UARS (Hays et al., 1993; Ortland et al., 1996). In addition, different types of ground-based radars deliver wind measurements of the upper atmosphere. Medium and low frequency radars determine wind by the drift of electron density irregularities which are sometimes detectable down to slightly below the mesopause (Briggs, 1980). Meteor radars measure the echoes from ionised particles in meteor trails drifting with the wind. Such particles are present in sufficient concentrations down to roughly 75 km (Jacobi et al., 2007). Additionally, it has been reported on the possibility of wind measurements by incoherent scatter radars reaching down to 60 km in the case of extraordinarily active auroral precipitation (Nicolls et al., 2010). Finally, ground-based lidars exploit returns from the atmospheric sodium layer to assess wind speeds between 85 and 100 km (Williams et al., 2004).

The region between 35 and 70 km where none of the previously described techniques is sensitive corresponds approximately to the so-called "radar gap" where radars do not detect usable echoes. Since the 1950ies atmospheric research rockets are used to bridge this gap by deploying falling targets to provide artificial radar backscatterers (National Research Council, 1966; Müllemann and Lübken, 2005) while wind measurements by optical tracking of a released chemical trace are generally limited to altitudes above 80 km (Larsen, 2002). However, as rocket-aided techniques are very expensive in costs they are only viable on campaign basis and not suited for continuous monitoring. A promising technique for observations in the gap region relies on lidar systems. Souprayen et al. (1999) described a horizontal wind climatology up to 50 km whereas the first lidar wind profiles covering the entire radar gap have been reported by Baumgarten (2010). However, the only dataset published from this instrument consists of a few days of polar night profiles (see also Hildebrand et al., 2012). Sensitivity of infrasound observations to the middle-atmospheric wind has been reported (e.g. Le Pichon et al., 2005a, b; Assink et al., 2014), but no full retrievals quantifying the wind speeds have yet been provided.

Microwave radiometry is sensitive to atmospheric emissions originating from the altitude range between 35 and 70 km where wind measurements are extremely scarce. This technique has a long history in measuring volume mixing ratio profiles of trace gases such as ozone or water vapor at these altitudes (e.g. Lobsiger et al., 1984; Lobsiger, 1987; Nedoluha et al., 1995, and references therein). Back in 1993 already, Clancy and Muhlemann (1993) had proposed the application of microwave radiometry for wind measurements in the middle atmosphere. One decade later Burrows (2007) and Flury et al. (2008) delivered the practical proof of the feasibility of such observations by measurements with an antarctic CO telescope and an airborne water vapour radiometer. These publications presented short data sets of average middle-atmospheric winds, whereas Rüfenacht et al. (2012) first reported on measurements of vertically resolved wind profiles in the upper stratosphere and mesosphere by a microwave radiometer operated as part of a regular measurement regime. Baron et al. (2013) later presented a data set comprising seven months of space-borne wind profile observations from SMILES. Unluckily, a technical failure stopped the operation of this instrument a few months before the ground-based wind radiometer WIRA recorded its first atmospheric observations so that there is no possibility for intercomparisons between the two instruments. Before the launch of SMILES, Wu et al. (2008) had described an approach for the retrieval of mesopause region wind profiles from the microwave limb sounder (MLS) on AURA.

Text S2. Figures. S3 and S4 are ~~analogons~~ analogs of Figs. 2 and 5 in the main article except that a pseudo-wavelet approach similar to the methods used in Studer et al. (2012) and Scheiben et al. (2014) was applied for the periodogram calculation. However, in the case of wind measurements, longer data gaps are present in the time series at some altitudes, therefore a more thorough treatment of those is necessary. Unlike in the cited studies data gaps were treated as missing values instead of being interpolated. Comparing Figs. S3 and S4 to Figs. 2 and 5 reveals only minor differences, hence both, the pseudo-wavelet and the Lomb-Scargle approach are suited for the spectral analysis of microwave remote sensing data.

Text S3. Figures ~~S4 to S11~~ S5 to S12 show the the periodograms of unaltered ECMWF data for all campaign sites and all time periods covered by the present study. Each figure covers the time interval of one measurement campaign. This additional data allows to better discriminate seasonal and latitude dependent effects from randomly occurring features.

Text S4. Figure~~S12~~ S13 presents the temporal evolution of the periodograms of WIRA data at the 0.05 hPa level. This corresponds to the altitude where Fig. 2 in the main article shows a minimum in the oscillation activity.

Text S5. Fig. S14 shows the campaign averages of the altitude dependent periodograms divided by the mean wind profile of the respective campaign for selected locations. Only zonal wind data from Bern, Sodankylä and Provence have been used beacuase the average zonal wind component from La Réunion as well as the average meridional components from Provence and La Réunion are close to zero so that a normalization would yield meaningless results. The agreement between ECMWF and WIRA becomes very good also for the upper altitudes when the periodogram is normalized by the average wind profile. This implies that the absolute wind speed discrepancy described in Rüfenacht et al. (2014) and the oscillation amplitude discrepancy increase in the same manner with increasing altitude.

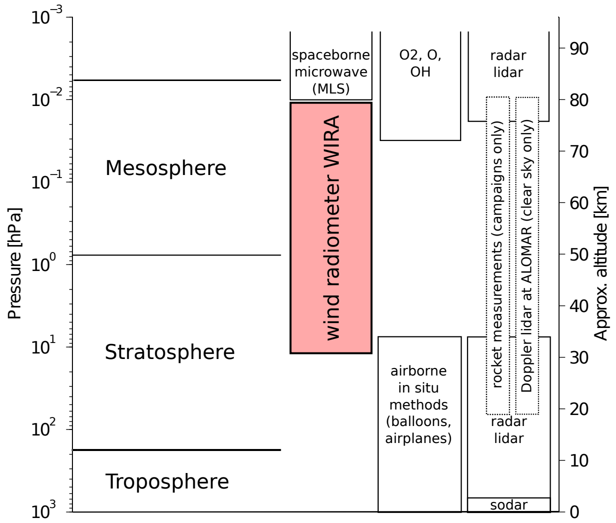

Figure S1. Overview of the existing techniques for wind observations with their typical sensitive altitude range. Under special atmospheric conditions extensions of the lower altitude limit of upper atmospheric incoherent scatter radars down to 60 km have been reported.

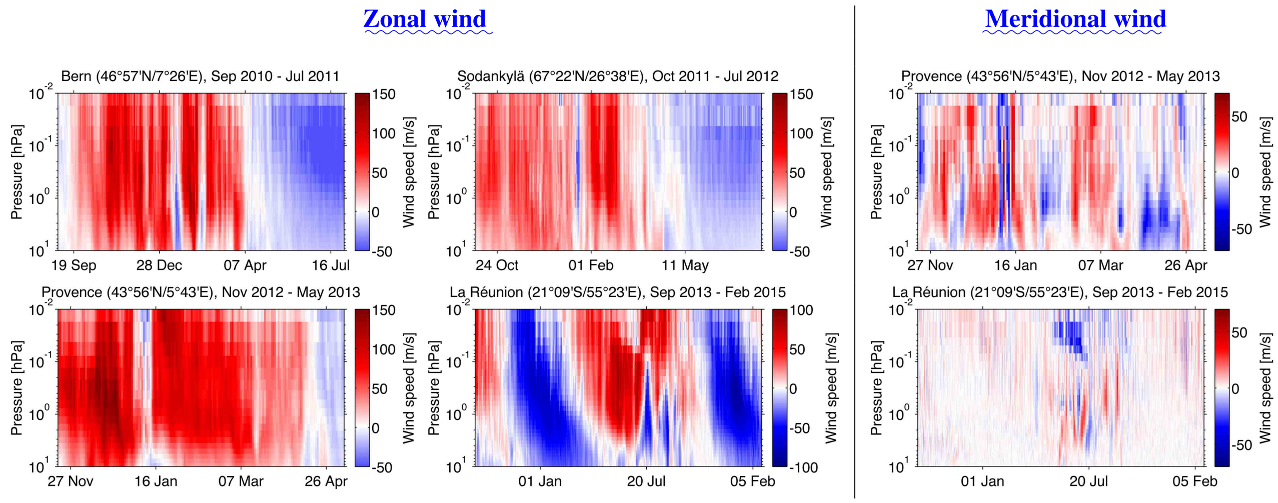

Figure S2. As Fig. 1 in the main article but for wind data from the ECMWF Operational Analysis.

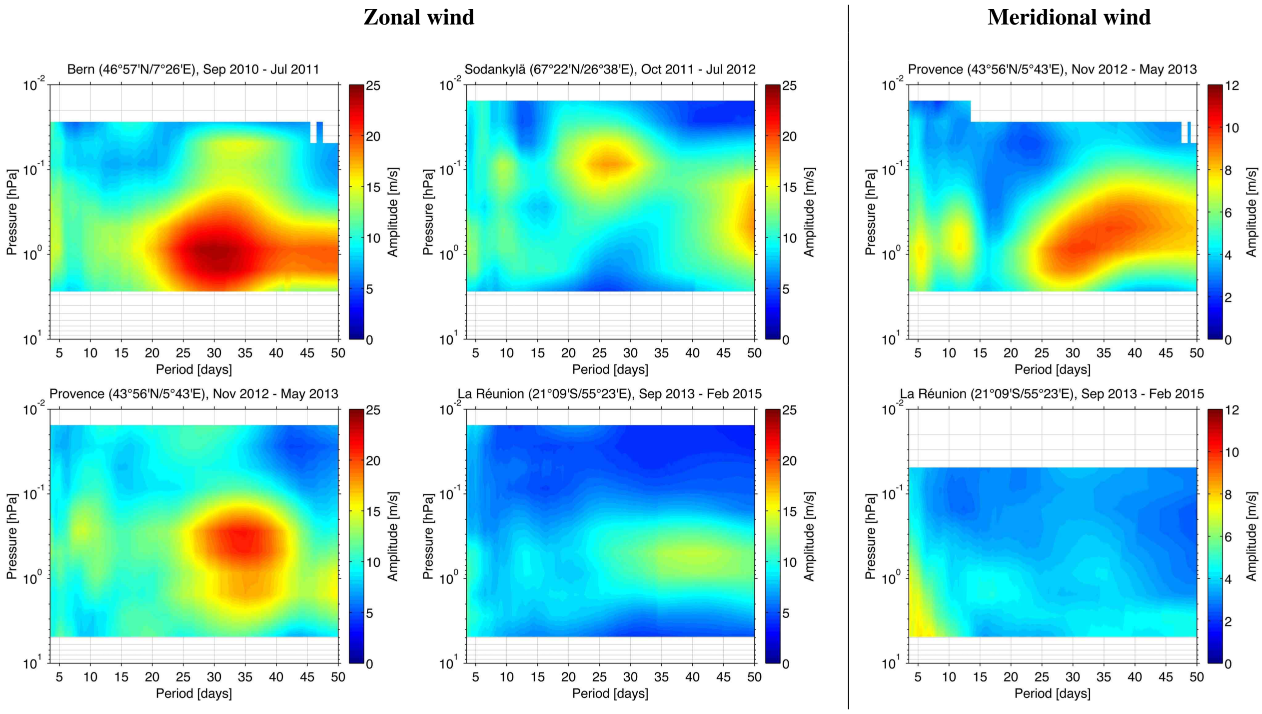

Figure S3. As Fig. 2 in the main article but for results obtained with the pseudo-wavelet approach.

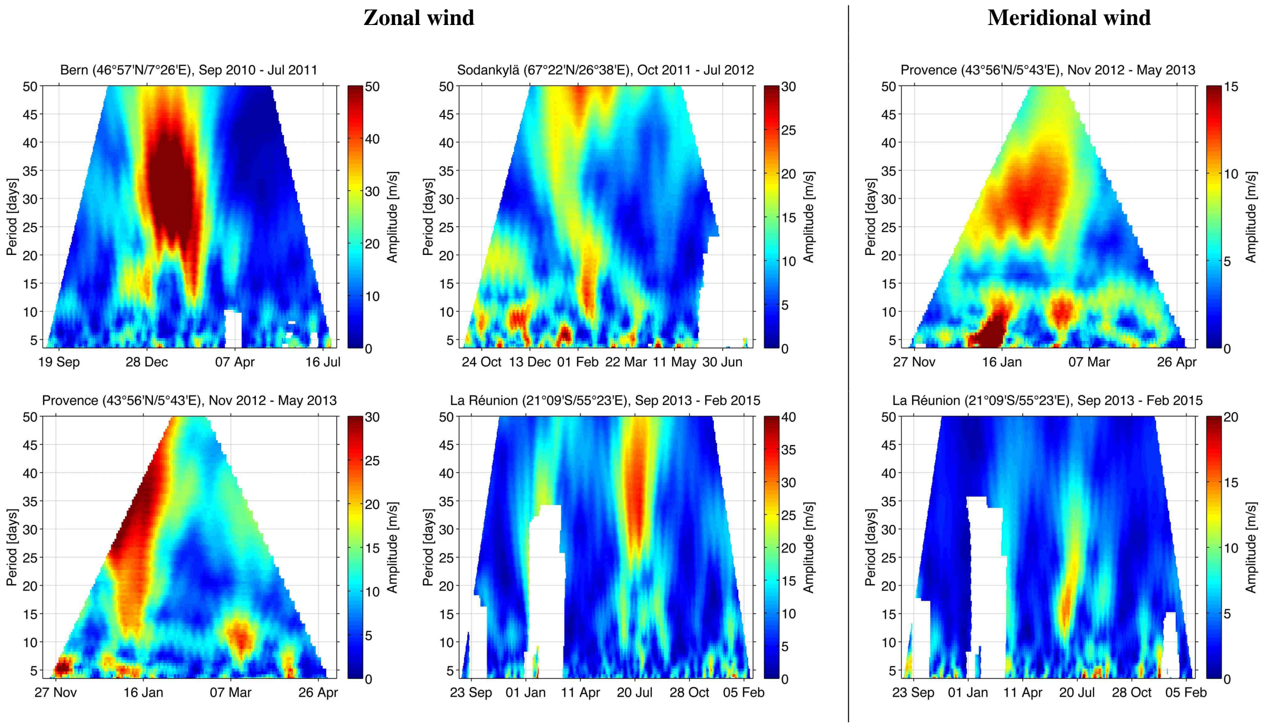

Figure S4. As Fig. 5 in the main article but for results obtained with the pseudo-wavelet approach.

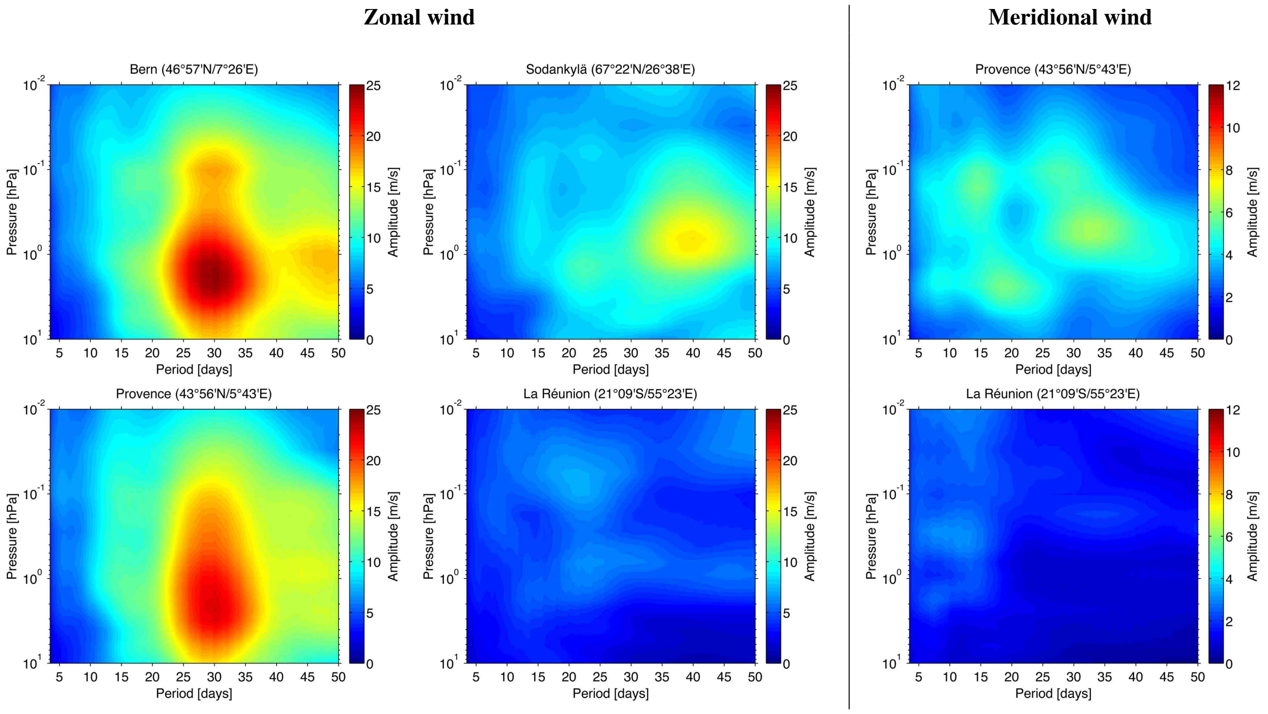

Figure S5. As Fig. 4 in the main article but with data for the time period 1 Sep 2010 - 31 Jul 2011 (time of the Bern campaign) for all locations.

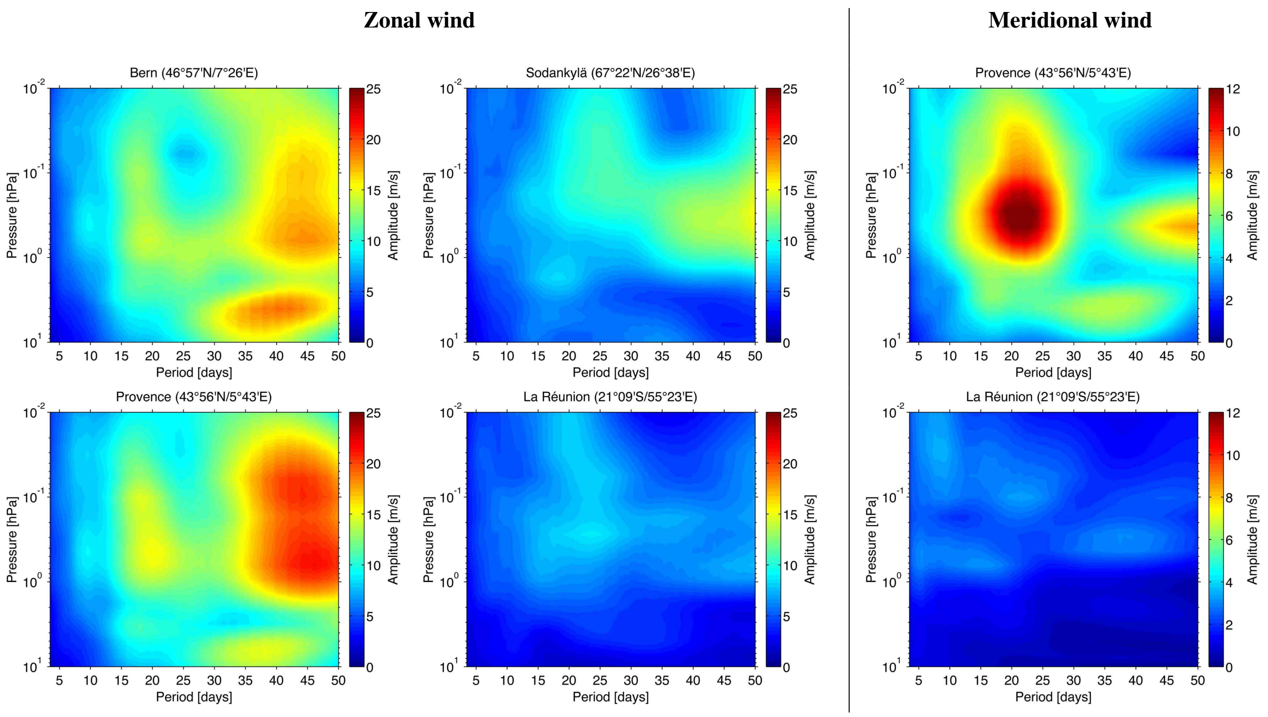

Figure S6. As Fig. 4 in the main article but with data for the time period 1 Oct 2011 - 31 Jul 2012 (time of the Sodankylä campaign) for all locations.

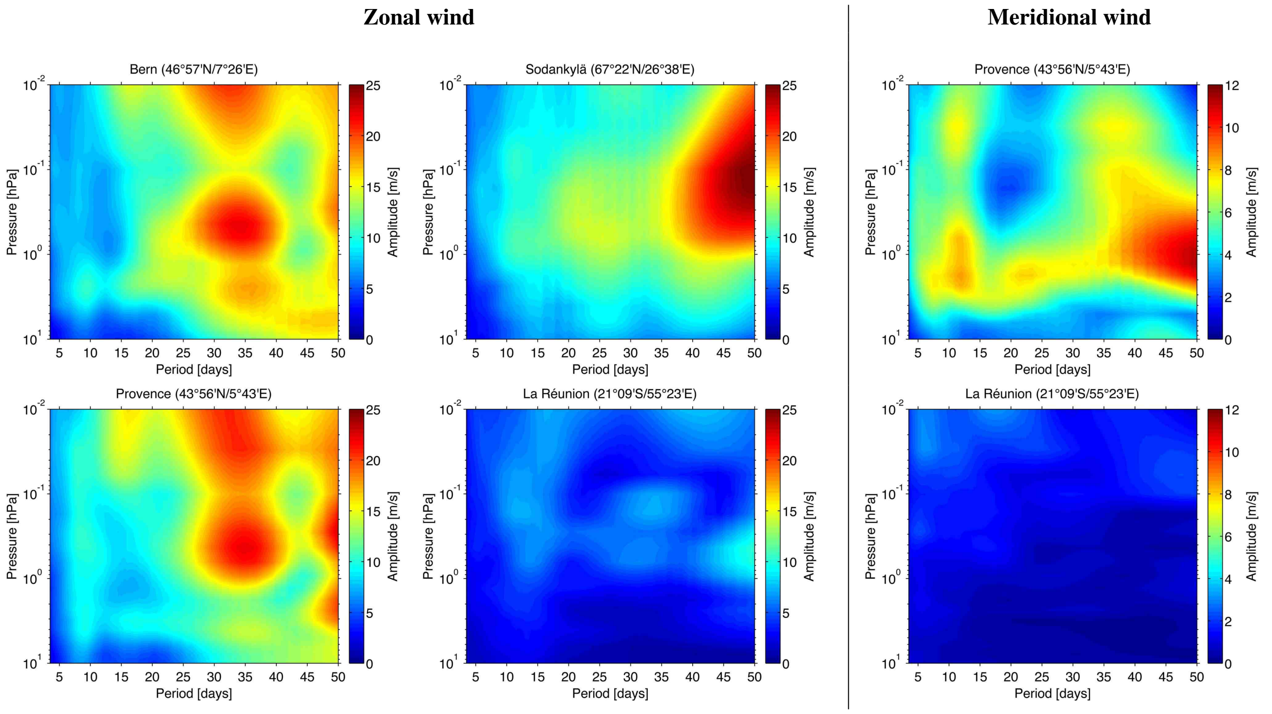

Figure S7. As Fig. 4 in the main article but with data for the time period 20 Nov 2012 - 6 May 2013 (time of the Provence campaign) for all locations.

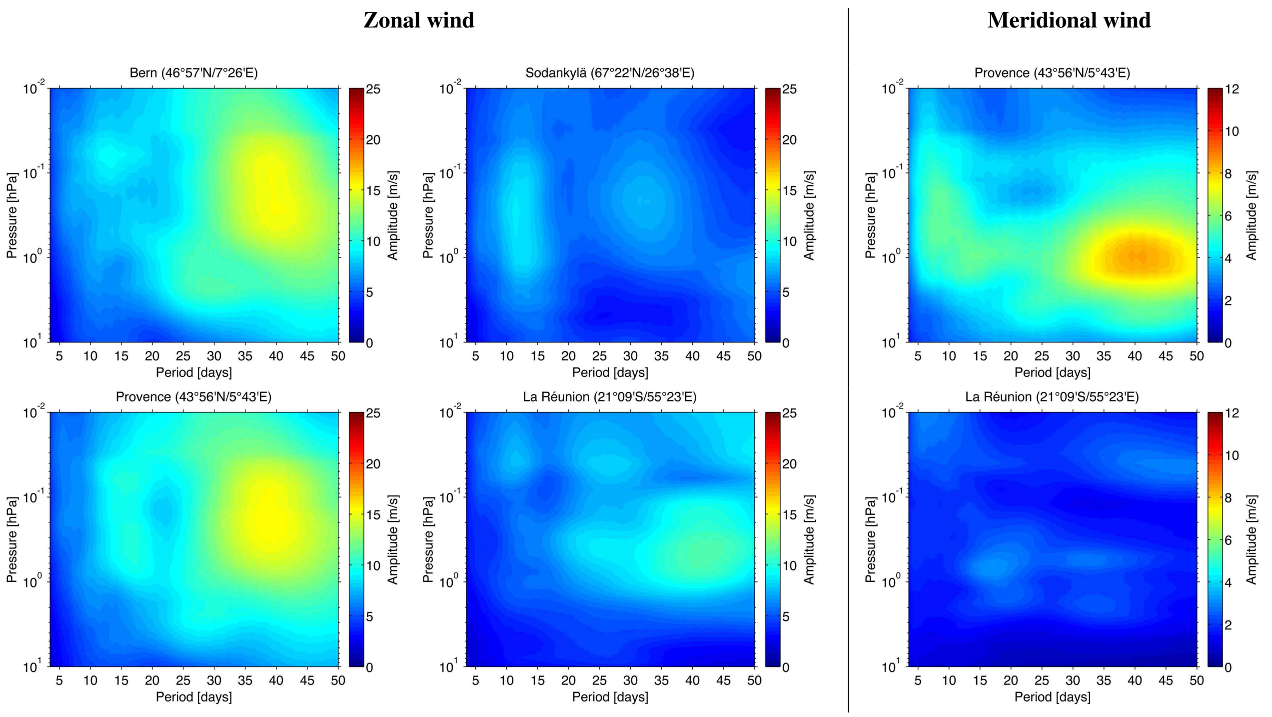

Figure S8. As Fig. 4 in the main article but with data for the time period 1 Sep 2013 - 21 Feb 2015 (time of the La Réunion campaign) for all locations.

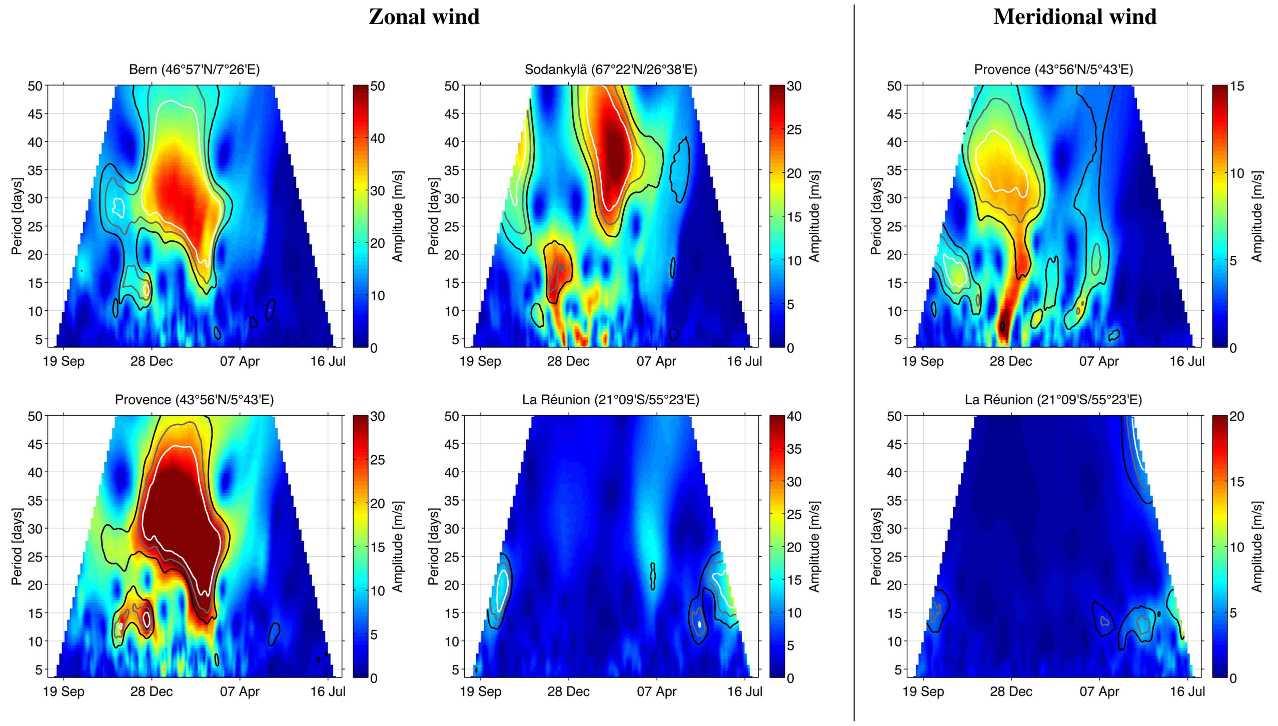

Figure S9. As Fig. 7 in the main article but with data for the time period 1 Sep 2010 - 31 Jul 2011 (time of the Bern campaign) for all locations.

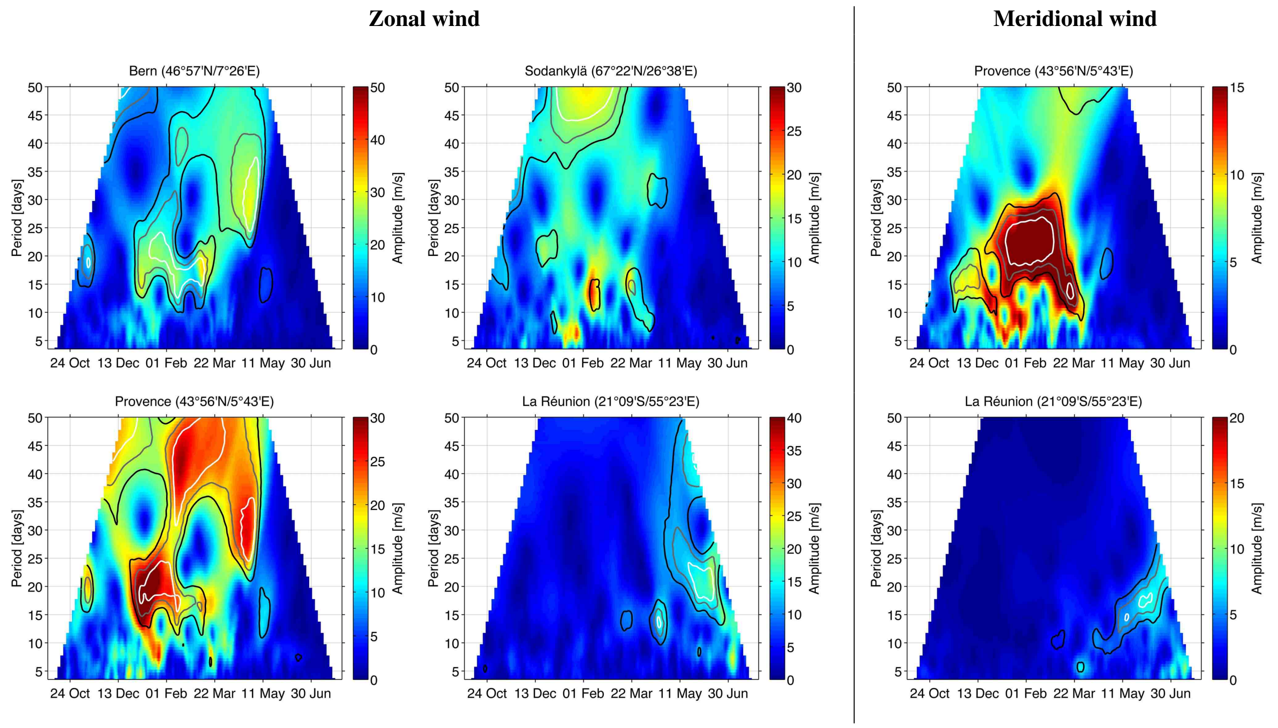

Figure S10. As Fig. 7 in the main article but with data for the time period 1 Oct 2011 - 31 Jul 2012 (time of the Sodankylä campaign) for all locations.

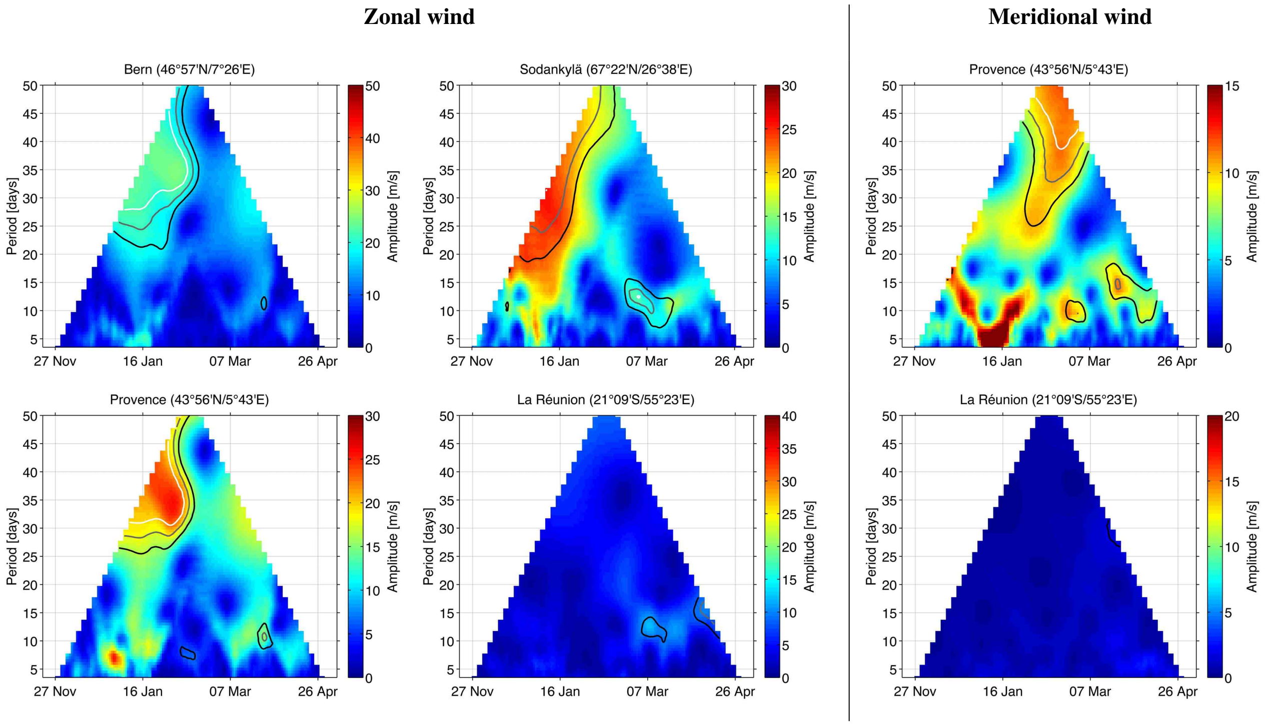

Figure S11. As Fig. 7 in the main article but with data for the time period 20 Nov 2012 - 6 May 2013 (time of the Provence campaign) for all locations.

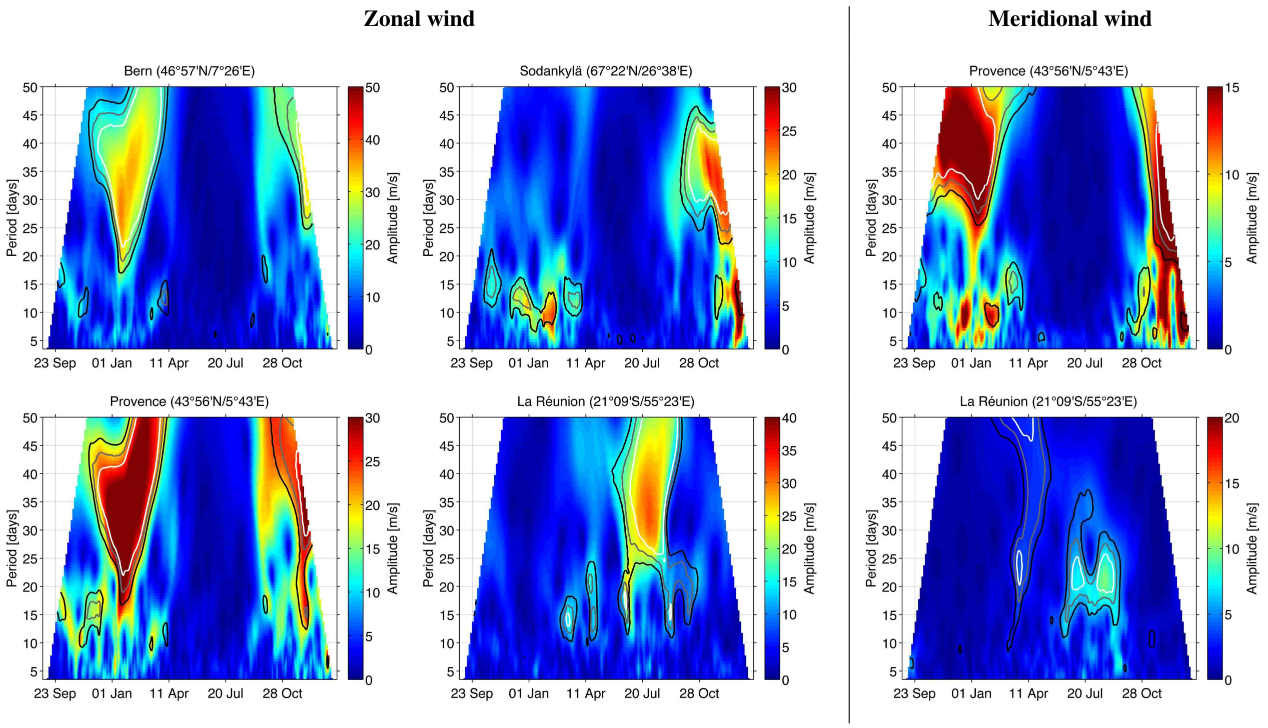

Figure S12. As Fig. 7 in the main article but with data for the time period 1 Sep 2013 - 21 Feb 2015 (time of the La Réunion campaign) for all locations.

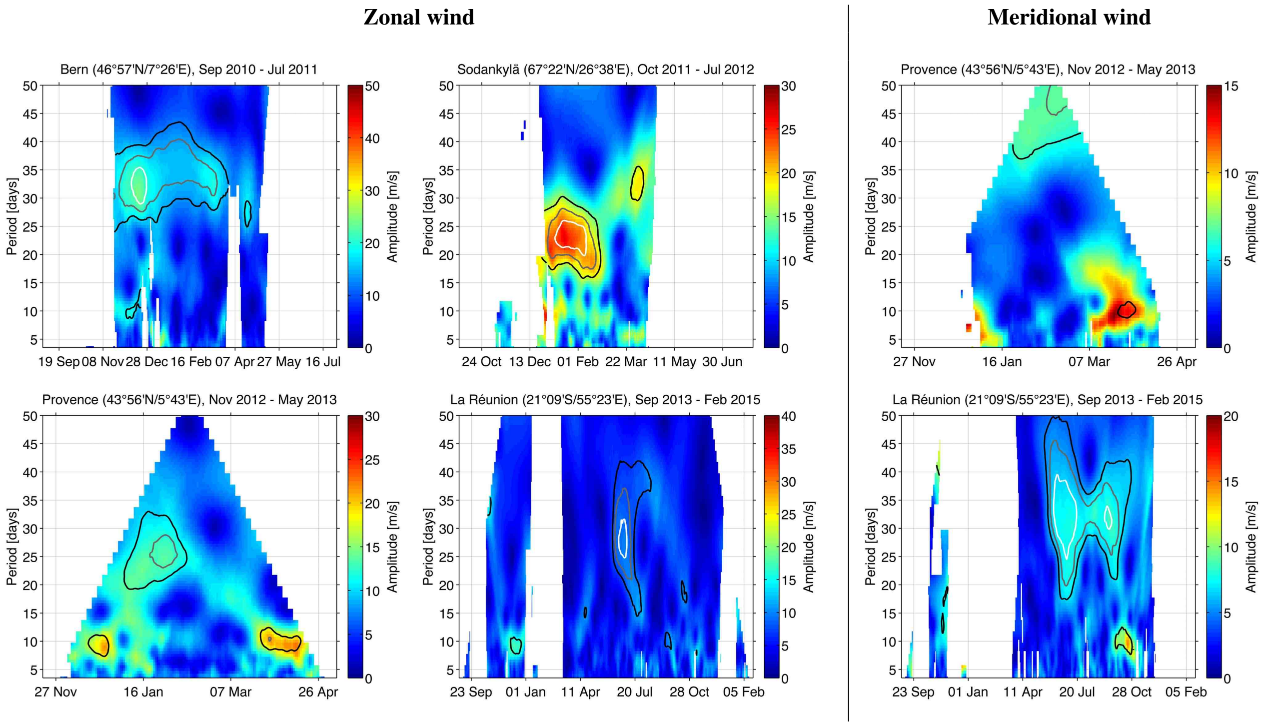

Figure S13. As Fig. 5 in the main article but for the temporal evolution of the WIRA periodogram at 0.05 hPa, which roughly corresponds to the altitude of minimal oscillation amplitudes. The color scale is identical to the plots at stratopause level.

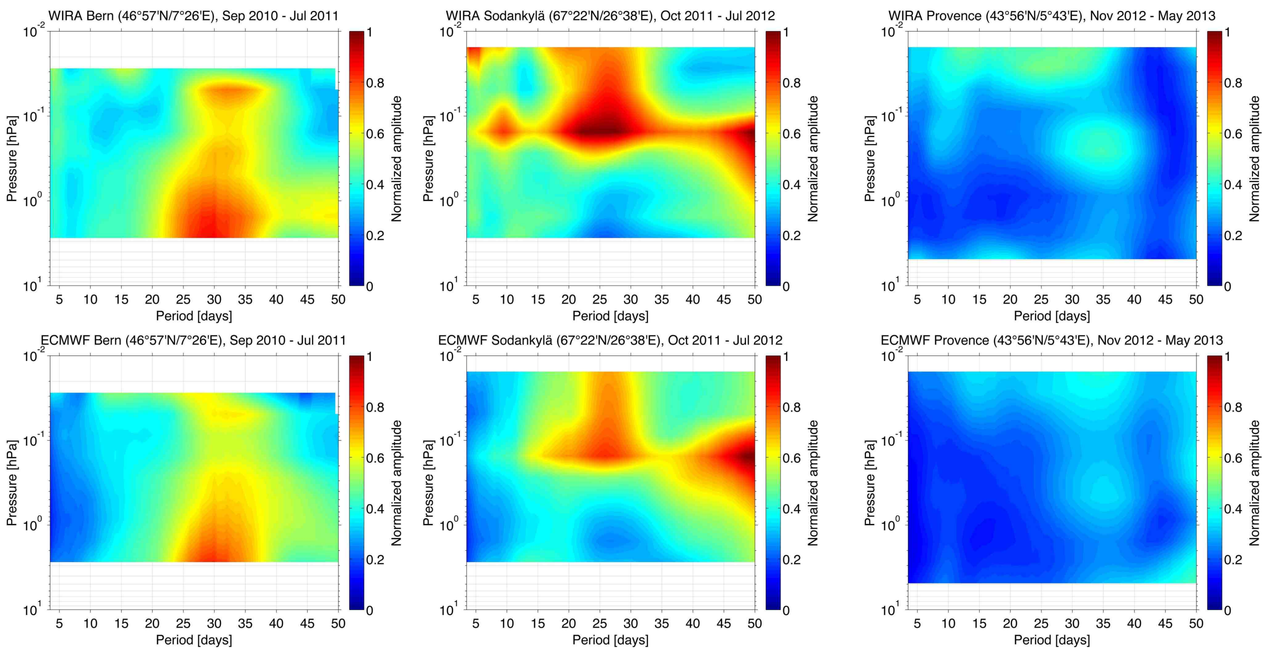

Figure S14. Temporally averaged periodograms of zonal and meridional wind profiles divided by the temporal average wind profile for the respective measurement campaigns. Results are shown for the zonal wind component in Bern, Sodankylä and Provence. Upper panels: WIRA; lower panels: ECMWF at WIRA.

References

Anandan, V. K., Kumar, M. S., and Rao, I. S.: First Results of Experimental Tests of the Newly Developed NARL Phased-Array Doppler Sodar, J. Atmos. Ocean. Technol., 25, 1778–1784, doi:10.1175/2008JTECHA1050.1, 2008.

Assink, J. D., Pichon, A. L., Blanc, E., Kallel, M., and Khemiri, L.: Evaluation of wind and temperature profiles from ECMWF analysis on two hemispheres using volcanic infrasound, J. Geophys. Res.-Atmos., 119, 8659–8683, doi:10.1002/2014JD021632, 2014.

Baron, P., Murtagh, D. P., Urban, J., Sagawa, H., Ochiai, S., Kasai, Y., Kikuchi, K., Khosrawi, F., Körnich, H., Mizobuchi, S., Sagi, K., and Yasui, M.: Observation of horizontal winds in the middle-atmosphere between 30° S and 55° N during the northern winter 2009-2010, Atmos. Chem. Phys., 13, 6049–6064, doi:10.5194/acp-13-6049-2013, 2013.

Baumgarten, G.: Doppler Rayleigh/Mie/Raman lidar for wind and temperature measurements in the middle atmosphere up to 80 km, Atmos. Meas. Tech., 3, 1509–1518, doi:10.5194/amt-3-1509-2010, 2010.

Briggs, B. H.: Radar observations of atmospheric winds and turbulence - a comparison of techniques, J. Atmos. Sol.-Terr. Phy., 42, 823–833, doi:10.1016/0021-9169(80)90086-0, 1980.

Burrows, S. M.: High-latitude remote sensing of mesospheric wind speeds and carbon monoxide, J. Geophys. Res.-Atmos., 112, doi:10.1029/2006JD007993, 2007.

Clancy, R. and Muhlemann, D.: Ground-based microwave spectroscopy of the Earth's stratosphere and mesosphere, in: Atmospheric Remote Sensing by Microwave Radiometry, edited by Janssen, M. A., chap. 7, pp. 372–374, John Wiley, 1993.

Elfving, A.: Aeolus – ESA's Wind Lidar Mission: Objectives, Design & Latest Results, Talk at Aeolus Cal/Val Workshop, 2015.

Flury, T., Hocke, K., Müller, S., and Kämpfer, N.: First measurements of lower mesospheric wind by airborne microwave radiometry, Geophys. Res. Lett., 35, doi:10.1029/2008GL034663, 2008.

Gault, W. A., Brown, S., Moise, A., Liang, D., Sellar, G., Shepherd, G. G., and Wimperis, J.: ERWIM: An E-region wind interferometer, Appl. Optics, 35, 2913–2922, doi:10.1364/AO.35.002913, 1996a.

Gault, W. A., Thuillier, G., Shepherd, G. G., Zhang, S. P., Wiens, R. H., Ward, W. E., Tai, C., Solheim, B. H., Rochon, Y. J., McLandress, C., Lathuillere, C., Fauliot, V., Herse, M., Hersom, C. H., Gattinger, R., Bourg, L., Burrage, M. D., Franke, S. J., Hernandez, G., Manson, A., Niciejewski, R., and Vincent, R. A.: Validation of O(S-1) wind measurements by WINDII: The WIND imaging interferometer on UARS, J. Geophys. Res.-Atmos., 101, 10 405–10 430, doi:10.1029/95JD03352, 1996b.

Gentry, B. M., Chen, H. L., and Li, S. X.: Wind measurements with 355-nm molecular Doppler lidar, Opt. Lett., 25, 1231–1233, doi:10.1364/OL.25.001231, 2000.

Goldberg, R. A., Fritts, D. C., Williams, B. P., Lübken, F.-J., Rapp, M., Singer, W., Latteck, R., Hoffmann, P., Mullemann, A., Baumgarten, G., Schmidlin, F.-J., She, C., and Krueger, D. A.: The MaCWAVE/MIDAS rocket and ground-based measurements of polar summer dynamics: Overview and mean state structure, Geophys. Res. Lett., 31, doi:10.1029/2004GL019411, 2004.

Hays, P. B., Abreu, V. J., Dobbs, M. E., Gell, D. A., Grassl, H. J., and Skinner, W. R.: The high-resolution doppler imager on the Upper Atmosphere Research Satellite, J. Geophys. Res.-Atmos., 98, 10 713–10 723, doi:10.1029/93JD00409, 1993.

Hildebrand, J., Baumgarten, G., Fiedler, J., Hoppe, U.-P., Kaifler, B., Lübken, F.-J., and Williams, B. P.: Combined wind measurements by two different lidar instruments in the Arctic middle atmosphere, Atmos. Meas. Tech., 5, 2433–2445, doi:10.5194/amt-5-2433-2012, 2012.

Hooper, D. A., Nash, J., Oakley, T., and Turp, M.: Validation of a new signal processing scheme for the MST radar at Aberystwyth, Ann. Geophys., 26, 3253–3268, doi:10.5194/angeo-26-3253-2008, 2008.

Jacobi, C., Froehlilch, K., Viehweg, C., Stober, G., and Kuerschner, D.: Midlatitude mesosphere/lower thermosphere meridional winds and temperatures measured with meteor radar, Adv. Space Res., 39, 1278–1283, doi:10.1016/j.asr.2007.01.003, 2007.

Killeen, T. L., Wu, Q., Solomon, S. C., Ortland, D. A., Skinner, W. R., Niciejewski, R. J., and Gell, D. A.: TIMED Doppler interferometer: Overview and recent results, J. Geophys. Res.-Space, 111, doi:10.1029/2005JA011484, 2006.

Larsen, M. F.: Winds and shears in the mesosphere and lower thermosphere: Results from four decades of chemical release wind measurements, J. Geophys. Res.-Space, 107, SIA 28–1–SIA 28–14, doi:10.1029/2001JA000218, 2002.

Le Pichon, A., Blanc, E., and Drob, D.: Probing high-altitude winds using infrasound, J. Geophys. Res.-Atmos., 110, doi:10.1029/2005JD006020, 2005a.

Le Pichon, A., Blanc, E., Drob, D., Lambotte, S., Dessa, J. X., Lardy, M., Bani, P., and Vergniolle, S.: Infrasound monitoring of volcanoes to probe high-altitude winds, J. Geophys. Res.-Atmos., 110, doi:10.1029/2004JD005587, 2005b.

Lobsiger, E.: Ground-based microwave radiometry to determine stratospheric and mesospheric ozone profiles, J. Atmos. Terr. Phys., 49, 493–501, doi:10.1016/0021-9169(87)90043-2, 1987.

Lobsiger, E., Künzi, K. F., and Dütsch, H. U.: Comparison of stratospheric ozone profiles retrieved from microwave-radiometer and Dobson-spectrometer data, J. Atmos. Terr. Phys., 46, 799–806, doi:10.1016/0021-9169(84)90060-6, 1984.

Luce, H., Fukao, S., Yamamoto, M., Sidi, C., and Dalaudier, F.: Validation of winds measured by MU radar with GPS radiosondes during the MUTSI campaign, J. Atmos. Ocean. Technol., 18, 817–829, doi:10.1175/1520-0426(2001)018<0817:VOWMBM>2.0.CO;2, 2001.

Müllemann, A. and Lübken, F.-J.: Horizontal winds in the mesosphere at high latitudes, Adv. Space Res., 35, 1890–1894, doi:10.1016/j.asr.2004.11.014, Coupling Processes in the MLT Region, 2005.

National Research Council: United States Space Science Program: Report to COSPAR, Ninth Meeting, National Academy of Sciences, 1966.

Nedoluha, G. E., Bevilacqua, R. M., Gomez, R. M., Thacker, D. L., Waltman, W. B., and Pauls, T. A.: Ground-based measurements of water vapor in the middle atmosphere, J. Geophys. Res.-Atmos., 100, 2927–2939, doi:10.1029/94JD02952, 1995.

Nicolls, M. J., Varney, R. H., Vadas, S. L., Stamus, P. A., Heinselman, C. J., Cosgrove, R. B., and Kelley, M. C.: Influence of an inertia-gravity wave on mesospheric dynamics: A case study with the Poker Flat Incoherent Scatter Radar, J. Geophys. Res.-

Atmos., 115, doi:10.1029/2010JD014042, 2010.

Ortland, D. A., Skinner, W. R., Hays, P. B., Burrage, M. D., Lieberman, R. S., Marshall, A. R., and Gell, D. A.: Measurements of stratospheric winds by the high resolution Doppler imager, Journal of Geophysical Research: Atmospheres, 101, 10 351–10 363, doi:10.1029/95JD02142, http://dx.doi.org/10.1029/95JD02142, 1996.

Rüfenacht, R., Murk, A., Kämpfer, N., Eriksson, P., and Buehler, S. A.: Middle-atmospheric zonal and meridional wind profiles from polar, tropical and midlatitudes with the ground-based microwave Doppler wind radiometer WIRA, Atmos. Meas. Tech., 7, 4491–4505, doi:10.5194/amt-7-4491-2014, 2014.

Rüfenacht, R., Kämpfer, N., and Murk, A.: First middle-atmospheric zonal wind profile measurements with a new ground-based microwave Doppler-spectro-radiometer, Atmos. Meas. Tech., 5, 2647–2659, doi:10.5194/amt-5-2647-2012, 2012.

Scheiben, D., Tschanz, B., Hocke, K., Kämpfer, N., Ka, S., and Oh, J. J.: The quasi 16-day wave in mesospheric water vapor during boreal winter 2011/2012, Atmos. Chem. Phys., 14, 6511–6522, doi:10.5194/acp-14-6511-2014, 2014.

Souprayen, C., Garnier, A., Hertzog, A., Hauchecorne, A., and Porteneuve, J.: Rayleigh-Mie Doppler wind lidar for atmospheric measurements. Instrumental setup, validation, and first climatological results, Appl. Optics, 38, 2410–2421, doi:10.1364/AO.38.002410, 1999.

Stoffelen, A., Marseille, G. J., Bouttier, F., Vasiljevic, D., de Haan, S., and Cardinali, C.: ADM-Aeolus Doppler wind lidar Observing System Simulation Experiment, Q. J. Roy. Meteor. Soc., 132, 1927–1947, doi:10.1256/qj.05.83, 2006.

Studer, S., Hocke, K., and Kämpfer, N.: Intraseasonal oscillations of stratospheric ozone above Switzerland, J. Atmos. Sol.-Terr. Phy., 74, 189 – 198, doi:10.1016/j.jastp.2011.10.020, 2012.

Williams, B. P., Fritts, D. C., Wang, L., She, C.-Y., Vance, J. D., Schmidlin, F. J., Goldberg, R. A., Mullemann, A., and Lübken, F.-J.: Gravity waves in the arctic mesosphere during the MaCWAVE/MIDAS summer rocket program, Geophys. Res. Lett., 31, doi:10.1029/2004GL020049, 2004.

Wu, D. L., Schwartz, M. J., Waters, J. W., Limpasuvan, V., Wu, Q., and Killeen, T. L.: Mesospheric Doppler wind measurements from Aura Microwave Limb Sounder (MLS), Adv. Space Res., 42, 1246–1252, doi:10.1016/j.asr.2007.06.014, 2008.